biospheremetrics v1.0.~~1~~.2: An R package to calculate two complementary terrestrial biosphere integrity indicators: human colonization of the biosphere (BioCol) and risk of ecosystem destabilization (EcoRisk)

Fabian Stenzel[1], Johanna Braun[1], Jannes Breier[1], Karlheinz Erb[2], Dieter Gerten[1,3,4], Jens Heinke[1], Sarah Matej[2], Sebastian Ostberg[1], Sibyll Schaphoff[1], and Wolfgang Lucht[1,3,4]

[1]Potsdam Institute for Climate Impact Research (PIK), Member of the Leibniz Association, P.O. Box 60 12 03, D-14412 Potsdam, Germany
[2]Institute of Social Ecology, University of Natural Resources and Life Sciences, Vienna (BOKU), Schottenfeldgasse 29, 1070 Vienna, Austria
[3]Humboldt-Universität zu Berlin, Department of Geography, Unter den Linden 6, D-10099 Berlin, Germany
[4]Integrative Research Institute on Transformations of Human-Environment Systems, Unter den Linden 6, D-10099 Berlin, Germany

Correspondence: Fabian Stenzel (stenzel@pik-potsdam.de)

Abstract. Ecosystems are under multiple stressors and impacts can be measured with multiple variables. Humans have altered mass and energy flows of basically all ecosystems on Earth towards dangerous levels. However, integrating the data and synthesizing conclusions is becoming more and more complicated. Here we present an automated and easy to apply R package to assess terrestrial biosphere integrity which combines ~~2~~ two complementary metrics:

5   (i) The BioCol metric quantifies the human colonization pressure exerted on the biosphere through alteration and extraction (appropriation) of net primary productivity, (ii) whereas the EcoRisk metric quantifies biogeochemical and vegetation structural changes as a proxy for the risk of ecosystem destabilization.

Applied to simulations with the dynamic global vegetation model LPJmL5 for 1500-2016, we find that presently (period 2007-2016), large regions show modification and extraction of >25% of the preindustrial potential net primary production~~, leading~~. The modification (degradation) of NPP as a result of land-use change and extraction in terms of biomass removal (from e.g. harvest) leads to drastic alterations in key ecosystem properties ~~and suggesting~~, which suggests a high risk for ecosystem destabilization. In consequence of these dynamics, EcoRisk shows particularly high values in regions with intense land use and deforestation, but also in regions prone to impacts of climate change such as the arctic and boreal zone.

The metrics presented here enable global-scale, spatially explicit evaluation of historical and future states of the biosphere
15   and are designed for use by the wider scientific community, not only limited to assessing biosphere integrity, but also to benchmark model performance.

The package will be maintained on GitHub and through that we encourage application also to other models and data sets.

Table 1. Abbreviations

BFT	bioenergy functional type
CFT	crop functional type
GCT	ground cover type
HANPP	human appropriation of NPP
LPJmL	Lund-Potsdam-Jena managed Land (a dynamic global vegetation model)
BioCol	metric for human biomass colonization pressure
EcoRisk	metric for risk of ecosystem destabilization
NPP	net primary production
PFT	plant functional type

1 Introduction

Earth system stability relies on functioning ecosystems (McKay et al., 2022), providing e.g. carbon sequestration, moisture
20 recycling, and resilience to disturbances/disruptions (Friedlingstein et al., 2022; Aragão, 2012; Oliver et al., 2015). The global
status and functioning of ecosystems is being evaluated using a range of approaches, including assessments of human footprint
(e.g. Venter et al. 2016), indicators based on empirically collected biodiversity data (e.g. Hudson et al. 2017; Newbold et al.
2016), or ecological computer models (e.g. Sakschewski et al. 2015).

Ecosystems depend on photosynthesis as major energy source, producing the primary biomass that is the foundation of
25 almost all food-webs. During the neolithic revolution, humanity decoupled its biomass demand from the natural cycle, which
led to large-scale modification of Earth's surface (Weisdorf, 2005). Today more than 75% of the ice-free land area of the Earth
is affected by human use (Watson et al., 2018; Arneth et al., 2019). However, the level of management and appropriation differs
widely from extensive (e.g. occasionally livestock-grazed steppes or extensively used forests) to intensive (e.g. machine-aided
agriculture with high mineral fertilizer use and irrigation). The aggregate effect of land use on ~~NPP~~net primary production
30 (NPP), i.e. altered productivity and removed biomass due to agricultural and forestry harvest, are often referred to as the
human appropriation of NPP (HANPP) (Haberl et al., 2004; Vitousek et al., 1986; Rojstaczer et al., 2001; Imhoff et al., 2004).
Utilizing this concept, it was shown that humanity has doubled its impact during the ~~20th~~ 20th century and thereby substantially
decreased the ~~net primary production (NPP)~~ NPP remaining in ecosystems (Krausmann et al., 2013; Kastner et al., 2022).

As one consequence of land use, only 40% of remaining forests are still characterized by high ecosystem integrity (Grantham
35 et al., 2020). Globally only 18.6% of highly intact habitats are currently protected (Mokany et al., 2020a), while modeling
pressure-impact relationships suggest an increasing mean species abundance loss until 2050, even under optimistic scenarios
with decreasing land use (Schipper et al., 2020; Williams et al., 2021). Over the course of this century, the dilemma of negative
effects from either climate change or climate change mitigation via large-scale biomass plantations highlights the need to
integrate biodiversity also in planning for negative emission technologies (Hof et al., 2018).

To prevent further degradation of the biosphere and to reverse current loss of nature, land use scenarios should take into account the regional risk for ecosystem destabilization (Rockström et al., 2021; Obura et al., 2022). As ecosystem destabilization we understand a severe change in ecosystem functioning, resulting in e.g. a decline in carbon sequestration, species composition, or water provisioning. Shifts in biogeochemical conditions can act as a proxy for this risk, based on the argument that substantial changes in either basic biogeochemical properties or vegetation composition are likely to imply far-reaching, potentially self-amplifying transformations in the underlying system characteristics, food chains and species composition (Heyder et al., 2011). The Γ-metric (Gamma), proposed by Heyder et al. (2011) represents such a metric, which has been used to separate the historical drivers of ecosystem change (Ostberg et al., 2015), compare the effects of climate warming and land use under future climate scenarios (Ostberg et al., 2018), and find temperature thresholds above which severe change is to be expected with high probability (Ostberg et al., 2013). Additionally, it has been applied component-wise to model outputs from the ISIMIP fast track ensemble, indicating an increasing area under risk of severe ecosystem change with rise of global mean temperature (Warszawski et al., 2013).

However HANPP cannot be modelled throughout, because it is based on census statistics and inventory data - modelling approaches have not been existing so far. On the other hand, the The original definition of Γ, however, did not include nitrogen variables and the code to compute it was hardly accessible to the scientific public. HANPP, on the other hand, so far was based on census statistics and inventory data and had not been calculated purely from vegetation model outputs.

We therefore propose an easy to apply R package with two complementary biosphere metrics, BioCol and EcoRisk, building on the existing indicators HANPP and Γ (Haberl et al., 2004; Heyder et al., 2011), which are here exemplarily calculated and evaluated based on simulations with the global vegetation model LPJmL5 (von Bloh et al., 2018).

BioCol quantifies the human colonization pressure on the biosphere through extraction of biomass and prevention of natural NPP by photosynthesis. The metric basically follows the HANPP approach by Haberl et al. (2007), who spatially explicitly sum extracted and inhibited biomass amounts based on biomass inventory data and compare them to potential NPP in a counterfactual world without human land use. We replace biomass inventory data with the corresponding LPJmL5 model outputs and thereby add the possibility to compute BioCol also from deep historical and future simulations.

EcoRisk illustrates state shifts of ecosystems as a result of land, water, and fertilizer use, as well as climate change based on the Γ-Metric (Heyder et al., 2011; Ostberg et al., 2015). It quantifies on the scale of 0 (no change) to 1 (very strong change) the dissimilarity of an ecosystem state from a reference condition and comprises 4 four subcomponents (vegetation structure, local change, global importance, ecosystem balance) that are aggregated as a multidimensional proxy for the risk of biosphere destabilization. We follow the original publications, but (additionally to water and carbon) now include nitrogen fluxes and pools. The addition of nitrogen variables fills a major gap, because nitrogen limitation or surplus is a key determinant for plant growth and the overall ecosystem status.

2 Material and methods

In this section, we detail the calculation of both metrics BioCol and EcoRisk, as well as our biome classification for spatial aggregation of results, and the relevant specifics of the vegetation model LPJmL5.

2.1 BioCol

75 We define BioCol (see Figure 1) as the flow of biomass (in terms of NPP) that is intentionally extracted in the form of crop, residue, and other biomass harvests (NPP_{harv}) plus the inhibited natural biomass production as a result of land use changes as well as management and differences in fires (NPP_{luc}). NPP_{luc} is calculated as the difference between potential natural NPP (i.e. the NPP that would prevail without land use but with current climate (Haberl et al., 2014) – NPP_{pot}) and the actual biomass production (NPP_{act}), both calculated under the same climate:

80
$$NPP_{luc} = NPP_{pot} - NPP_{act} \tag{1}$$

Using time series of NPP_{pot} and NPP_{act} allows to remove the climate change (e.g. CO_2 fertilization) effect in the component NPP_{luc}. NPP_{luc} can become negative, if the actual NPP is higher than potential NPP (e.g. through management or land use legacy effects, especially on managed grasslands). Absolute HANPP and relative $BioCol$ are computed as

$$HANPP = NPP_{luc} + NPP_{harv} \tag{2}$$

85 where NPP_{harv} denotes the NPP withdrawn from ecosystems via harvest.

$$BioCol = HANPP/NPP_{ref} \tag{3}$$

where NPP_{ref} represents a reference NPP. In earlier applications, the respective NPP_{pot} of each year has been used as reference (Kastner et al., 2022; Krausmann et al., 2013). In contrast, we here use NPP_{ref}, which refers to the NPP_{pot} of the pre-industrial period (mean of 1550-1579), which is the same timeframe as for EcoRisk. NPP_{harv} sums the corresponding
90 LPJmL5 model outputs for harvested and extracted carbon from crop areas (including residues), second generation biomass plantations (not existing in historical period land use input) and grassland, as well as timber harvests from land use conversion, combined with external timber extraction from managed forests, and human induced fire carbon emissions. Residue harvest was assumed to contain 70% of the remaining above-ground biomass after harvest. Carbon extraction on grasslands includes carbon contained in dairy products and methane emissions plus respiration and is based on prescribed livestock densities
95 (Heinke et al., 2023), which are calibrated to match grazing amounts for the year 2000 originally provided by Herrero et al. (2013) and modified by Heinke et al. (2020) (about 1.1 GtC/yr globally). Currently, LPJmL5 is not able to model managed forests, and also does not separate human induced and lightning induced fire carbon emissions. Therefore, timber harvest from managed forests is included as an external dataset from LUH2-v2h (Hurtt et al., 2020). Human induced fire carbon emissions can be included through external data on the human fire ignition fraction of total fire carbon emissions, based on fire models
100 such as LPJmL-Spitfire (Thonicke et al., 2010). For this study, the fire carbon emissions are not included, since the updated
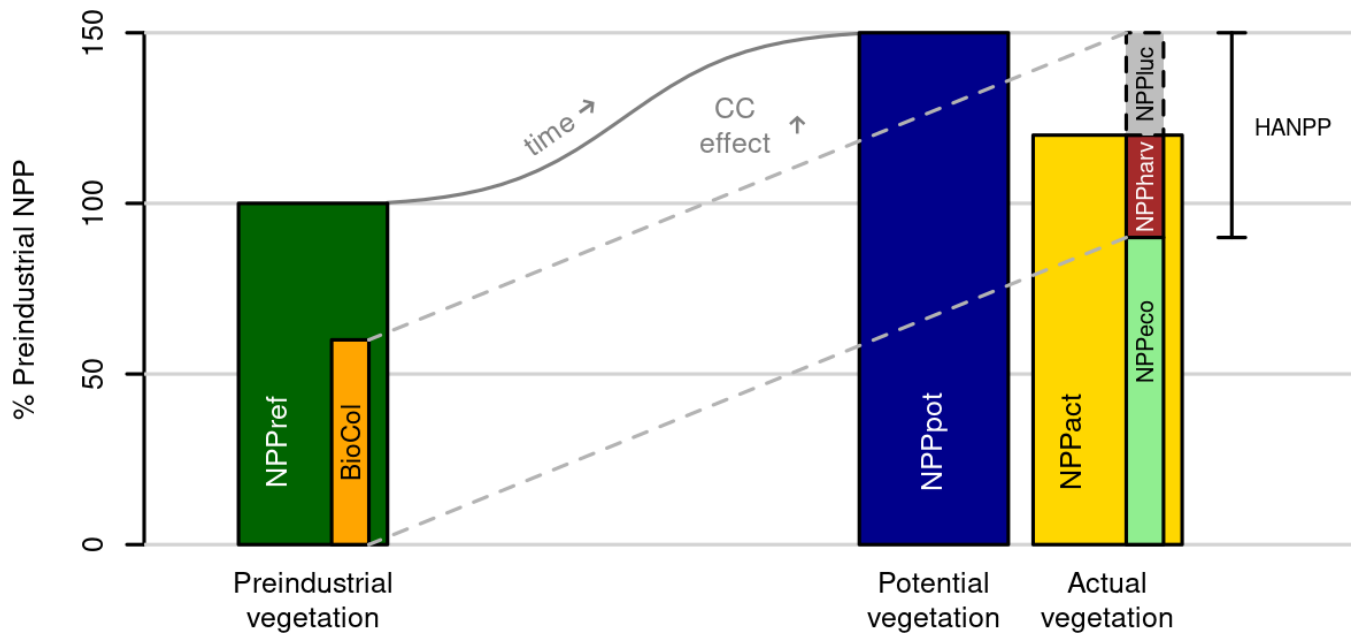
Figure 1. Calculation scheme for BioCol. The basis for our analysis is the preindustrial potential NPP (NPP$_{ref}$) assessed from 1550-1579. The effects of CO_2 fertilization of plants resulting from historical anthropogenic CO2 emissions, changes in atmospheric N deposition, and climate change lead to a net increase in NPP today (labeled as the "CC effect" in the biosphere), both for hypothetical "Potential vegetation" without human land use and the "Actual vegetation" including land use. HANPP is calculated as the sum of direct human biomass extraction (NPP$_{harv}$) and inhibited natural productivity through replacing natural vegetation with land use (NPP$_{luc}$ = NPP$_{pot}$ - NPP$_{act}$). BioCol is subsequently computed as the fraction of HANPP compared to NPP$_{ref}$.

LPJmL-Spitfire version is still being tested.

$$\text{human fire ignition fraction} = \frac{\text{human ignitions}}{\text{human ignitions} + \text{lightning ignitions}} \quad (4)$$

NPP_{pot}, representative of the NPP under potential natural vegetation (under transient climate), is obtained from a model simulation without human land use, but otherwise identical settings to the run providing NPP_{act}. $BioCol$ or HANPP and sub-components are available as spatially explicit values per grid cell for every timestep, but also as global sums over time, or aggregated per biome or world region. When aggregating grid-cell values of BioCol, negative values can be treated as such, reducing the overall pressure, or the absolute values of all grid-cells can be summed up (which is mainly used in this analysis). For further details on the LPJmL5 simulation setup, see subsection 2.5.

2.2 EcoRisk

EcoRisk is computed as the average of four subcomponents: vegetation structure (vs), local change (lc), global importance (gi), and ecosystem balance (eb), each on the same scale of 0 to 1 and internally scaled with the respective change-to-variability

ratio $S(x, \sigma_x)$, following Ostberg et al. (2018):

$$\text{EcoRisk} = \frac{vs \ + \ lc \ + \ gi \ + \ eb}{4} = \frac{V \cdot S(V, \sigma_V) + l \cdot S(l, \sigma_l) + g \cdot S(g, \sigma_g) + e \cdot S(e, \sigma_e)}{4} \tag{5}$$

The unscaled **vegetation structure** component V is evaluated based on the dissimilarity of the vegetation composition of the whole grid cell for both natural and managed areas based on Sykes et al. (1999); Heyder et al. (2011); Ostberg et al. (2018). For this, LPJmL5 provides outputs of the ground area covered by natural and cultivated plant types. Changes in vegetation structure are computed between ecosystem state i and j with respect to the total area (G) of ground cover type (GCT) k (tree, grass, or barren), further detailed by the differences between the plant functional type (PFT) (p) specific area (A) regarding attribute l (evergreenness, needleleavedness, tropicalness, borealness, naturalness). For PFT specific attributes (a) see Table 2. Barren is defined without subcategories. The attribute specific weighting factor ω_{kl} is per default set to 0.2 (= "equal" weighting). Alternatively, attribute specific weights as in Ostberg et al. (2018) can be applied.

$$V(i,j) = 1 - \sum_k \left\{ \underbrace{\min\left(G_{ik}, G_{jk}\right)}_{total\ area\ of\ GCT\ k} \cdot \left[1 - \sum_l \left(\omega_{kl} \underbrace{\left| \sum_p (A_{iklp} \cdot a_{klp}) - \sum_p (A_{jklp} \cdot a_{klp}) \right|}_{specific\ area\ difference\ regarding\ attribute\ l} \right) \right] \right\} \tag{6}$$

The remaining components l, g, and e are computed from two ecosystem state vectors $\boldsymbol{s}_1$ (reference state) and $\boldsymbol{s}_2$ (changed state), composed of 30 year averages of biogeochemical variables $v_{1,i}$ and $v_{2,i}$, with $i = [1, ..., n]$.

$$\boldsymbol{s}_1 = \begin{pmatrix} v_{1,1} \\ \vdots \\ v_{n,1} \end{pmatrix}, \boldsymbol{s}_2 = \begin{pmatrix} v_{1,2} \\ \vdots \\ v_{n,2} \end{pmatrix} \tag{7}$$

They represent the major process cycles on the grid cell level determining plant growth: carbon, nitrogen, and water. The system described by the metric is the terrestrial land system, which has pools as well as in- and outfluxes across the system boundary. For carbon and nitrogen, stocks are aggregated into a vegetation and soil pool, for water there is only a soil pool. In total this gives 11 dimensions, plus one dimension reserved for other relevant processes (for LPJmL filled with the fire fraction) (Table 3). The user can define which model output variables constitute each process dimension. Hereby it is important, to know the model specific details to keep consistency. If possible, output variables should use per-area units because of the per area weighting for the "global importance" component.

Local change describes changes compared to the local reference state (e.g. the preindustrial time) as the magnitude change of the difference vector of the biogeochemical properties (how strongly the local conditions have changed). For this, the state variables are normalized with the local values of the reference state:

$$\boldsymbol{s}_{l_1} = \begin{pmatrix} 1 \\ \vdots \\ 1 \end{pmatrix}, \ \boldsymbol{s}_{l_2} = \begin{pmatrix} v_{1,l} \\ \vdots \\ v_{n,l} \end{pmatrix} \tag{8}$$

Table 2. PFT specific attributes a_{klp} for GCTs tree and grass.

trees	evergreenness	needleleavedness	tropicalness	borealness	naturalness
Tropical broadleaved evergreen	1	0	1	0	1
Tropical broadleaved raingreen	0	0	1	0	1
Temperate needleleaved evergreen	1	1	0	0	1
Temperate broadleaved evergreen	1	0	0	0	1
Temperate broadleaved summergreen	0	0	0	0	1
Boreal needleleaved evergreen	1	1	0	1	1
Boreal broadleaved summergreen	0	0	0	1	1
Boreal needleleaved summergreen	0	1	0	1	1
Tropical bioenergy	1	0	1	0	0
Temperate bioenergy	0	0	0	0	0

grasses/crops	tropicalness	borealness	naturalness
C4 grass tropic	1	0	1
C3 grass temperate	0	0	1
C3 grass polar	0	1	1
Temperate cereals	0	0	0
Rice	1	0	0
Maize	1	0	0
Tropical cereals	1	0	0
Pulses	0.5	0	0
Temperate roots	0	0	0
Tropical roots	1	0	0
Sunflower	0.5	0	0
Soybean	1	0	0
Groundnut	1	0	0
Rapeseed	0.5	0	0
Sugarcane	1	0	0
Others	0.5	0	0
Managed grass	dyn*	dyn*	0
Bioenergy grass	1	0	0
Grass under bioenergy trees	dyn*	dyn*	0

* dynamic share due to climate specific grass mix

Table 3. Processes and associated variables describing the land system and their aggregation from LPJmL5 outputs.

Process description	LPJmL5 variable(s)	Relevance for ecosystem
vegetation structure		
surface area covered	Natural vegetation and bioenergy: foliage projected cover	available plant groups
by respective plant groups	Crops: land use fraction	and their surface coverage
carbon pools		
vegetation carbon pool	vegetation carbon	carbon stored in vegetation
soil carbon pool	soil carbon + litter carbon	carbon stored in soil
carbon fluxes		
carbon influx	GPP	source of exergy for ecosystem
carbon outflux	autotrophic respiration + heterotrophic respiration	carbon losses
	+ fire carbon emissions + harvested carbon (crops+residues)	
nitrogen pools		
vegetation nitrogen pool	vegetation nitrogen	nitrogen stored in vegetation
soil mineral nitrogen pool	soil NH_4^+ + soil NO_3^-	reactive nitrogen stored in soil
nitrogen fluxes		
nitrogen influx	biological nitrogen fixation + fertilizer nitrogen input	nitrogen entering the system
	+ manure nitrogen input + atmospheric nitrogen deposition	
nitrogen outflux	harvested nitrogen (crops+residues) + nitrogen leaching to surface water	nitrogen leaving the system
	+ N_2O emissions from denitrification and nitrification	
	+ N_2 emissions + nitrogen volatilization + fire nitrogen emissions	
water pool		
soil water pool	root zone soil moisture	available green water
water fluxes		
water influx	precipitation + irrigation	sources of water
water outflux	plant transpiration + soil evaporation + interception + runoff	sinks of water
other		
other processes	fire frequency	other ecosystem-relevant processes

with

$$v_{i,l} = \frac{v_{i,2}}{v_{i,1}}, \text{ for } v_{i,1} \neq 0. \tag{9}$$

For variables, which are 0 in both vectors, both are set to 1, resulting in no change. If only the reference case is 0, the unscaled values are used for both vectors.

Global importance, in contrast, puts these local changes in perspective to the global mean reference condition, taking into account that even moderate changes on the local scale may feed back to larger scales if large enough in absolute terms. Therefore, the state vectors are normalized with the global, spatially averaged reference mean value $\overline{v_{i,refg}}$:

$$\boldsymbol{s}_{g_1} = \begin{pmatrix} v_{1,g,1} \\ \vdots \\ v_{n,g,1} \end{pmatrix}, \; \boldsymbol{s}_{g_2} = \begin{pmatrix} v_{1,g,2} \\ \vdots \\ v_{n,g,2} \end{pmatrix} \tag{10}$$

with

$$v_{i,g,t} = \frac{v_{i,t}}{\overline{v_{i,refg}}}, \text{ for } \overline{v_{i,refg}} = \frac{1}{\sum a_p} \sum_{p=1}^{z} a_p v_{i,p} \neq 0. \tag{11}$$

for cells $p = 1, ..., z$ with cell area a_p. If the global mean reference state is 0, instead the mean scenario state is used for scaling. If both are 0, both vectors are set to 1, as for local change. Afterwards both state vectors for global importance and local change are multiplied by $\frac{1}{\sqrt{n}}$ to scale it down according to the number of variables (EcoRisk can also be computed for simulations without nitrogen, and thus missing the corresponding variables). The difference between the two states is now characterized by the length of the difference vector between them, which for local change and global importance are defined as:

$$d_l = |\boldsymbol{s}_{l_2} - \boldsymbol{s}_{l_1}|, \; d_g = |\boldsymbol{s}_{g_2} - \boldsymbol{s}_{g_1}| \tag{12}$$

Ecosystem balance quantifies shifts in the relative magnitude of biogeochemical properties with respect to each other as an indicator for qualitative changes in the balance of dynamic processes, which may signal a breakdown of ecological functioning (Ostberg et al., 2018). It is calculated from the angle between the two state vectors with local normalization (as for local change):

$$b' = 1 - cos(\alpha) = 1 - \frac{\boldsymbol{s}_{l_1} \cdot \boldsymbol{s}_{l_2}}{|\boldsymbol{s}_{l_1}||\boldsymbol{s}_{l_2}|} \tag{13}$$

b' is scaled to a range between 0 and 1 assigning a value of 1 if the angle between state vectors is larger than $60°$:

$$e = \begin{cases} b' \cdot 2 & \text{if } \alpha \leq 60°, \\ 1, & \text{otherwise} \end{cases} \tag{14}$$

Values for metric components l and g are derived by scaling d_l and d_g to a range between 0 and 1 using the ~~following~~ sigmoid transformation function T:

$$l = T(d_l), \; g = T(d_g), \quad T(x) = A + \frac{1 - A}{1 + e^{-6(x-0.5)}} \tag{15}$$

$$T(x) = A + \frac{1-A}{1 + e^{-6(x-0.5)}}$$

with $A = -\frac{1}{e^3}$.

The year-to-year variability is accounted for by the **change-to-variability ratio**. This variability factor is based on the standard deviation (σ_x) of the component in the 30 year reference period, based on the assumption that ecosystems are adapted to the variability they are regularly exposed to but may be vulnerable if it is exceeded. The change-to-variability ratio $S(x, \sigma_x)$ for components $x \in (V, l, g, e)$ is calculated as

$$S(x, \sigma_x) = \frac{1}{1 + e^{-4(\frac{x}{\sigma_x} - 2)}} \tag{16}$$

with σ_x the interannual standard deviation of x under reference conditions.

For the specific status of variables describing the same process (e.g. carbon pools, or water fluxes), the change metric is also evaluated only for those variables, per default as $(lc + gi + eb)/3$, but for compatibility with earlier applications, it is possible to only use lc.

2.3 Comparison to other indicators

To contextualize EcoRisk and BioCol with other biosphere integrity indicators, we transformed a set of ~~7~~ seven widely used biosphere integrity indicators (Table 4) to the interval [0,1] (with 0 meaning high integrity/no pressure/low risk) and show them alongside EcoRisk and BioCol, together with scatterplots of EcoRisk and BioCol against the average value across all indicators. We additionally extracted thresholds for each indicator from the literature, that demarcate the transition between the low and high risk zone (sources listed in Table 4). With these, we calculated the number of indicators per grid cell, that show up as transgressed.

2.4 Biome classification

To aggregate BioCol and EcoRisk from grid cells to the biome level (to also enable analysis for these larger-scale ecological units), we updated the biome classification for LPJmL5, originally published by Ostberg et al. (2013). It is based on the vegetation structure and its fractional coverage per cell, tree specific leaf area index, temperature, and the carbon stored in vegetation. Cells are classified primarily based on the total tree cover. Thresholds of 60%, 30% and 10% are chosen to demarcate the boundaries between forests, woody savanna/woodland, savanna, and grassland based on the IGBP land cover classification system (Belward, 1996). The dominant tree or grass species then determines the type of biome. Compared to Ostberg et al. (2013), the thresholds can be adjusted and an additional differentiation between Tropical Rainforest and warm woody Savanna/Woodland can be either based on the tree leaf area index, or the vegetation carbon (in this paper, we use a tree leaf area index of 6 as threshold). Additionally, Montane Grassland can be differentiated from Arctic Tundra by elevation or latitude (here, we use an elevation threshold of ~~1000m). Today's biomes are classified as shown in .~~ 1000 m).

Table 4. Sources for other biosphere integrity indicators and associated thresholds.

Indicator	range	source	threshold	threshold source
GLASOD: degree of human induced soil degradation	1-4	Oldeman et al. (1990)	strong/extreme: >2	Oldeman et al. (1990)
HF: human footprint	[0,50]	Venter et al. (2018)	high pressure: >6	Venter et al. (2016)
BII: biodiversity intactness index	[0.5,1]	Newbold et al. (2016)	BII target: >0.8	Soergel et al. (2021)
intactness: GLOBIOM 2015 MSA https://portal.geobon.org	[0,1]	Schipper et al. (2020)	degraded: <0.6	visual inspection
FLII: Forest Landscape Intactness Index	[0,10]	Grantham et al. (2020)	low integrity: 0-6	Grantham et al. (2020)
CI: contextual intactness	[0,1]	Mokany et al. (2020a)	high-value: >0.5	Mokany et al. (2020b)
CoE: Convergence of Evidence from World Atlas of Desertification wad.jrc.ec.europa.eu/geoportal	[0,10]	Cherlet et al. (2018)	many: >7	Cherlet et al. (2018)

2.5 LPJmL5

We employ the dynamic global vegetation model LPJmL 5.7 (Schaphoff et al., 2018; von Bloh et al., 2018), which can be run
195 standalone (forced by climate inputs) or coupled into the Potsdam Earth Model POEM (Drüke et al., 2021).

LPJmL5 simulates key ecological and physiological processes such as photosynthesis, respiration, carbon allocation and turnover for natural and managed vegetation based on historical data or future projections of land use, soil, nitrogen inputs, and climate conditions. The composition of natural vegetation, represented by 11 PFTs, dynamically develops based on climatic parameters, growth efficiency, competition and fire disturbance (Sitch et al., 2003), while agricultural crop composition is
200 prescribed considering 12 crop functional types (CFTs) (Bondeau et al., 2007), grassland/pastures (Heinke et al., 2023), and three second-generation bioenergy crop functional types (BFTs) (Beringer et al., 2011). The remaining group of "other" crops is simulated as temperate wheat or tropical maize, depending on the latitude. CFT specific sowing dates are dynamically calculated based on optimal season length and fixed after the year 2000 (Waha et al., 2012). Local runoff is routed through a global network of water bodies and river channels as accumulated discharge (Gerten et al., 2004). Irrigated crop area is
205 prescribed, but irrigation requirements and water withdrawals are dynamically simulated based on the soil water deficit and available renewable water in lakes, rivers, reservoirs as well as neighboring cells with available water (Jägermeyr et al., 2015).

Different agricultural management practices and their impacts on soil processes and yields are simulated, including tillage, manure, and fertilizer application as well as optional growth of off season cover crops (Lutz et al., 2019; Porwollik et al., 2022). Fluxes and stocks of carbon, nitrogen and water are by default resolved on $0.5°$x$0.5°$ spatial and daily time scale. For this study all outputs are aggregated per year.

Output from LPJmL5 to compute BioCol and EcoRisk is read and processed using the R package lpjmlkit (Breier et al., 2023).

We ran the model with a fused climate input from the ISIMIP project (GSWP3-W5E5). It combines daily GSWP3 data from 1901 to 1978 with a bias-adjusted version of ERA5 (W5E5, adjusted to better match CRU and GPCC) from 1979 to 2016 (Kim, 2017; Lange, 2019). Manure, fertilizer, and crop specific cultivation areas from 1500 to 2018 are taken from a new hybrid dataset (Ostberg et al., 2023). Fallow land was included in the CFT class "others", while the distribution of irrigated area into irrigation systems is based on Jägermeyr et al. (2015). Livestock densities on grasslands were determined based on estimates of grazing levels at both regional and production system levels reported by Herrero et al. (2013), using a set of simulation presented by Heinke et al. (2023). Tillage input is based on Lutz et al. (2019). For simulation years before 1901, the first 30 years of the climate input are randomly recycled.

3 Results

The results of BioCol are (except for forest harvest) strictly model-based and are in general well in line with the existing data-based assessments (Kastner et al., 2022; Krausmann et al., 2013). The global sum of HANPP, based on LPJmL5 simulated outputs, increases from below 2 [2.5] GtC/yr before 1700 to more than 13 [15] GtC/yr today, depending on whether the absolute values are summed up for cells with negative values or not (Figure 2a - left y-axis). Over the course of the ~~20th~~ 20th century, relative values of BioCol thus approximately doubled from about 0.1 to over 0.2 (10% to over 20%) compared to the potential preindustrial NPP$_{ref}$ of the ~~16th~~ 16th century (Figure 2a - right y-axis). Since 2000 the values increased further. When taking the absolute for negative cells, BioCol is approaching 0.25 (25%) in 2016 – meaning that almost a quarter of the total terrestrial preindustrial biomass production on Earth is rerouted to human use or inhibited compared to a world without humans.

The global relative BioCol pattern for the year 2000 (1995-2005 average) shows high values for areas of intense agricultural use (Figure 2b). The abundance of cells with negative BioCol values (higher productivity in the simulation with land use than in the similar run with only potential natural vegetation) might be explained by the explicit simulation of agricultural management especially in regions with low natural NPP (e.g. irrigation in the Middle East) and potential legacy effects from earlier land use on now natural areas included in our land use dataset (e.g. in the Amazon, NPP upon regrowth of natural vegetation on abandoned agricultural areas is simulated to be higher than potential NPP in the equilibrium state; see Figure A1).

Isolated cells with very high absolute BioCol values (e.g. in the Boreal zone) are locations of reservoirs established before the year 2005, with associated decline in NPP and thus high values of NPP_{luc}.
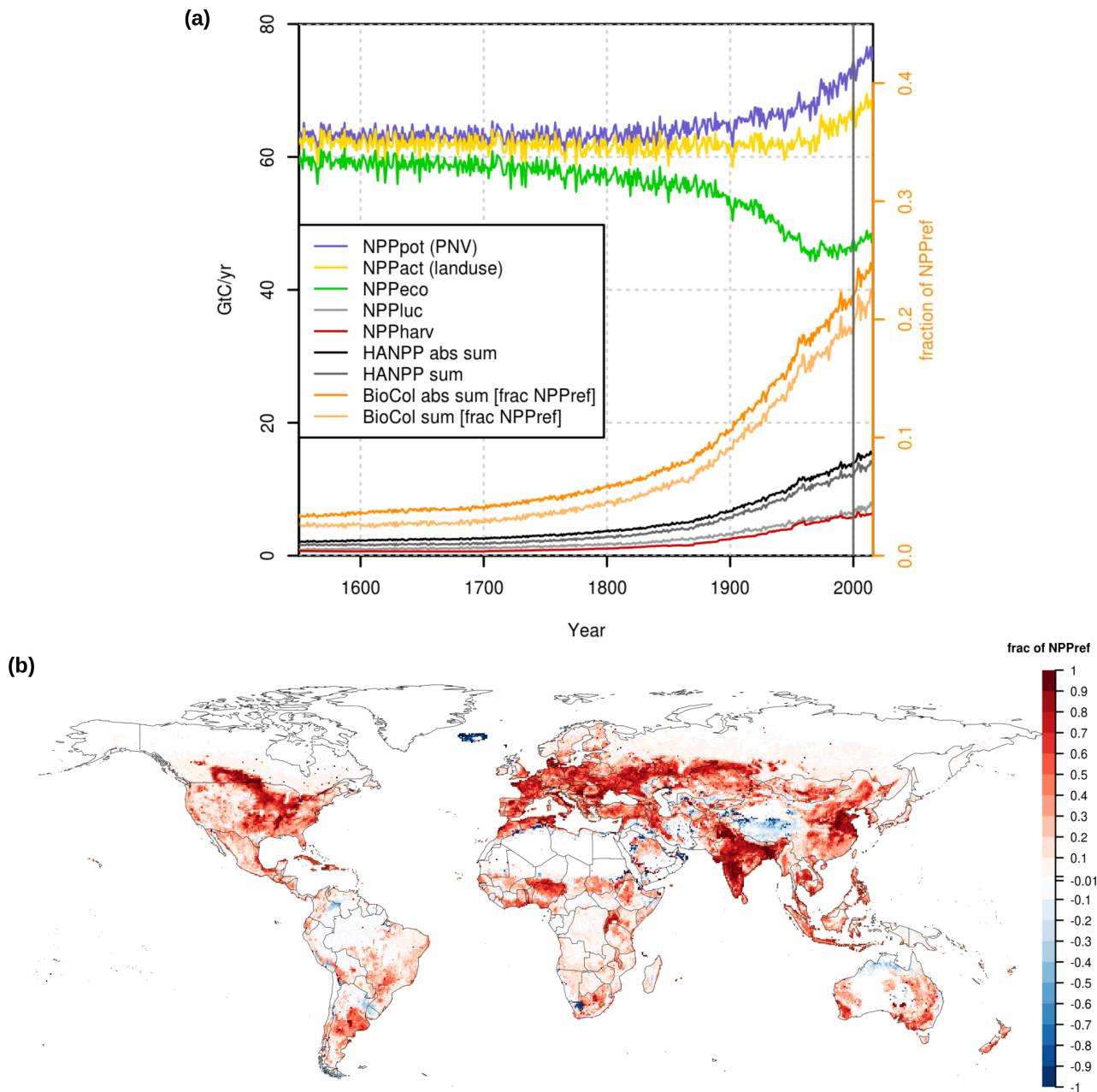
Figure 2. (a) Global BioCol and components over time. **(b)** ~~map~~ Map of the relative values for the year 2000 (average 1995-2005). Relative values for BioCol are expressed in comparison to the average NPP from 1550-1579 from a run without human land use.

EcoRisk calculated between 1550-1579 and 1985-2016 shows large areas with values above 0.5 (Figure 3), mostly in regions with high land use intensity today. Land use change is reflected in the vegetation structural change component (vs), which resembles quite closely the current land use extent (see inlet). However the components building on changes in biochemical

variables (lc, gi, eb) indicate a much larger extent of region with values > 0.9. Figure 4b and Figure A2 show that in many regions changes in nitrogen fluxes are responsible for these strong changes.

Climatic changes are also reflected in EcoRisk. They are most visible in the components ecosystem balance (eb) and vs as bands of higher values along the frontier of boreal vegetation onset to the North in Canada. In Eurasia (and other land use free regions of the Arctic) this vegetation shift appears more patchy. The local change component (lc) indicates high values among especially vulnerable ecosystems with low absolute values (arctic, deserts), which do not show up in the global importance (gi). ~~gi primarily shows high values~~ Values of gi are high in regions with strong absolute changes, e.g. with intense land use, or loss of tropical rainforests. Ostberg et al. (2018) provides a more detailed discussion of separate and combined effects of land use and climate change (however for a somewhat differently defined metric and using an earlier model version and different input database).

For the original Γ-metric, a threshold of 0.3 had been established, which indicates the transition from moderate to high risk of ecosystem destabilization. To determine whether this threshold is still valid for EcoRisk (given the adaptations to the computation, particularly the inclusion of nitrogen flows and pools which show more variability), we performed two sets of synthetic simulations. We assume that a meaningful threshold should meet the following two criteria: (i) it should be higher than internal variability within biomes, but (ii) lower than the variability between distinct biomes, such that a simulated EcoRisk above this threshold is indicative of changes equivalent to a shift in biome. For (i) we checked the homogeneity within forest biomes, by computing EcoRisk with values from 1550-1579 between each cell of a biome and the average cell of this biome. In all forest biomes, internal biome variability for at least half the cells is higher than 0.3 compared to the average biome cell (Figure A3). Thus, values of < 0.5 could better describe most of the internal variation.

For (ii), we compared the average biome cells against each other by computing EcoRisk between the current states of each of them. Most combinations show EcoRisk values > 0.3, when compared against each other (Figure A4), with some exceptions: Boreal Needleleaved Evergreen Forest is classified as relatively similar to Temperate Broadleaved Deciduous Forest (0.26), a fact that we cannot explain - and also complicated by the reverse direction showing a high value of 0.62. Tropical Rainforest is classified as similar to Tropical Deciduous Forest. This can be partially explained through their similar locations and overlap in species. Arctic Tundra and Montane Grassland are classified as similar. They are in fact the same biome, but at different elevation. Comparably, Temperate Savanna, Temperate Woodland and Warm Grassland are classified as similar biomes, only differentiated by total tree cover fraction and C3/C4 grass shares. There are further biomes which show intermediate values of $0.3 <$ EcoRisk < 0.5 when compared against each other, all partially explainable through compositional similarity or similar average conditions.

However, Figure A4 also highlights that EcoRisk is not symmetric, mainly because of the normalization to different reference conditions for local change and ecosystem balance. Strong directional discrepancies can for example be observed for the difference between the three biomes "Temperate Needleleaved Evergreen Forest", "Temperate Broadleaved Deciduous Forest", and "Boreal Needleleaved Evergreen Forest".

Aggregating EcoRisk grid cell values to the biome level, according to the biome classification yields three classes (Figure 4): ~~1~~(i) Those with a median EcoRisk < 0.3: "Tropical Rainforest", "Tropical Deciduous Forest", "Boreal Broadleaved Deciduous
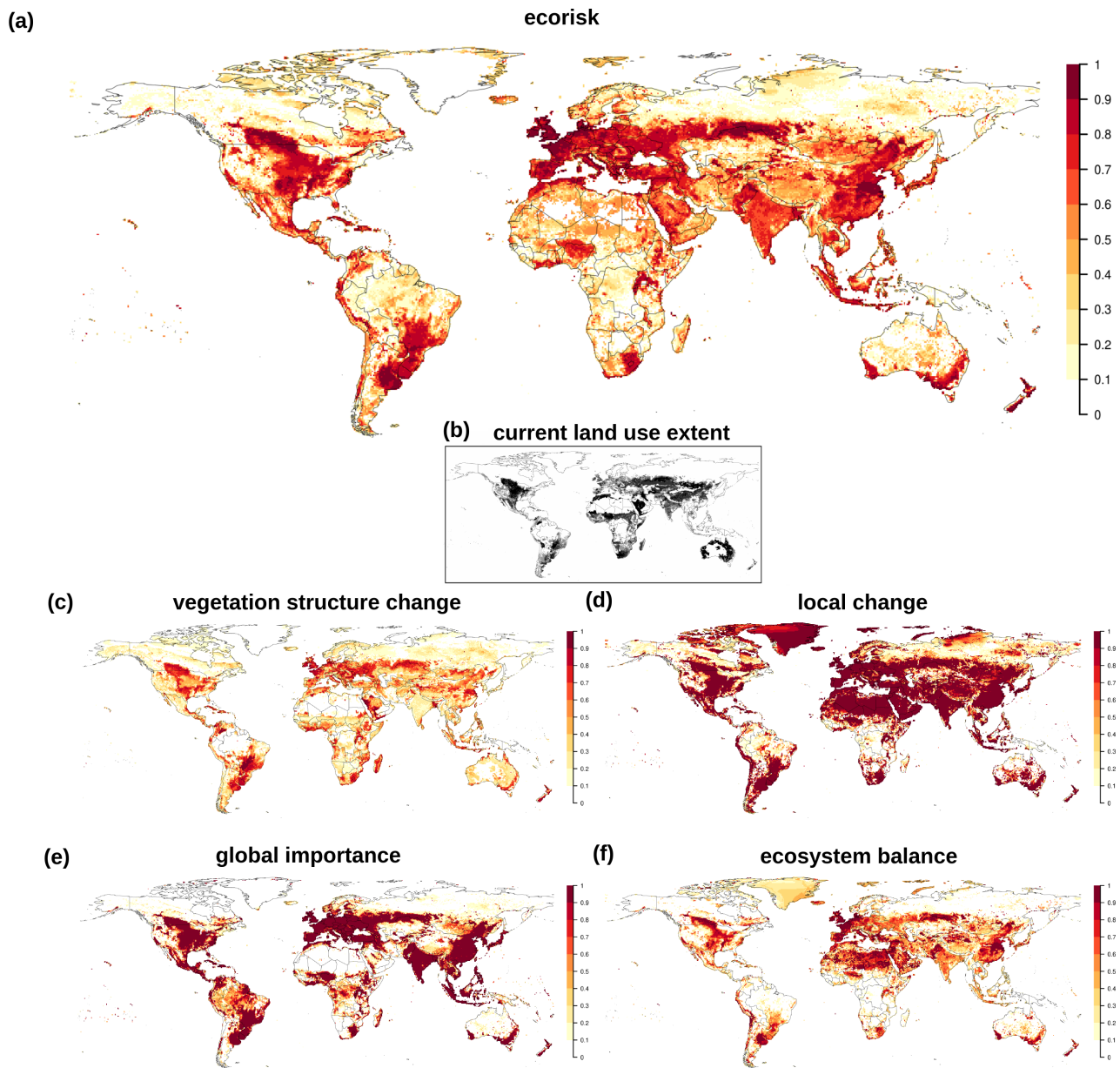
Figure 3. **(a)** Change in biochemical compositions computed by EcoRisk between 1550-1579 and 1985-2016. **(b)** current land use extent for reference. **(c-f)** EcoRisk components: vegetation structure change, local change, global importance, ecosystem balance

Forest", "Boreal Needleleaved Deciduous Forest" (only few cells), "Arctic Tundra" - 2̶(ii) those with 0.3 < median EcoRisk < 0.65: "Boreal Needleleaved Evergreen Forest", "Warm Woodland", "Warm Savanna", "Warm Grassland", "Temperate Savanna", "Temperate Grassland", "Montane Grassland", "Desert" - and 3̶(iii) those with a median EcoRisk > 0.65: "Temperate Broadleaved Deciduous Forest", "Temperate Needleleaved Evergreen Forest", "Temperate Woodland". The subcomponent lo-

cal change is generally the one with highest values (except for TrRF, TrDF, BoND) and nitrogen fluxes in all cases show stronger changes than those for carbon and water.

Comparison of EcoRisk and BioCol with other biosphere integrity indicators (Table 4), shows similar trends despite high scattering (Figure 5k,m). The maps highlight that the pattern of BioCol is more similar to that of other transgressed indicators (Figure 5a-j), however this might stem from most of them being directly affected by land use. The additional benefit of EcoRisk is that it also captures effects due to climate and deposition changes.

4   Discussion

We present a model-based indicator set that allows to assess the state of the biosphere. We show that presently (period 2007-2016), large regions show modification and extraction of >25% of the preindustrial potential net primary production according to the indicator BioCol, along with climatic changes leading to drastic alterations in key ecosystem properties and suggesting a high risk for ecosystem destabilization according to the indicator EcoRisk.

Generally the indicators presented in this package can serve both as an analytic tool to assess biosphere integrity from model simulations, or for means of benchmarking model performance (e.g. after new development). Therefore depending on the context, the performance of the vegetation model is important. This paper primarily describes the methodology behind the biospheremetrics package, with the application to model results only being secondary. LPJmL5 is currently in a recalibration and validation phase, with major changes to code and key processes, following the implementation of tillage and the nitrogen cycle. Further model development may particularly focus on an improved distribution of PFTs and thus biomes (see Harper et al. 2023 for comparison) and the explicit simulation of multi-cropping, which has been neglected here. A better representation of human induced fire emissions and including process based forest management will also be important, since the effects on NPP are currently not considered.

The next step for us is thus to extend the biospheremetrics package to be compatible with other vegetation models (e.g. utilizing outputs from the ISIMIP3 ensemble) and thus also allow for intermodel comparison.

As presented in the previous section, the addition of nitrogen fluxes leads to a strong increase in values for EcoRisk, when comparing to earlier results of the Γ-Metric (Figure 3, Figure A2 and Ostberg et al. 2015, 2018). Relative changes in nitrogen fluxes (Figure A5) as a result of nitrogen fertilizer and manure application are much stronger than those for carbon and water fluxes and pools (Figure A6, Figure 4). This is intuitively plausible, however the question remains, whether the associated high values for EcoRisk mainly resulting from the relative changes in nitrogen fluxes really correspond to a strongly increased risk for ecosphere destabilization. Generally, a theory of how changes in different components (vs, lc, gi, eb) or classes of state variables (e.g. water pools or nitrogen fluxes) can be translated to risk of ecosphere destabilization is lacking (and could be different among components/classes). Theoretically, a weighted downscaling of any component would be possible, however the literature base for such changes is currently lacking. We thus refrained from any weighting until further research is done on this end.

The results for EcoRisk show a strong increase in the overall values. A new threshold between moderate and high risk (replacing 0.3 in Ostberg et al. 2018, 2015; Heyder et al. 2011) would be as high as 0.48, when picking the "optimal" EcoRisk threshold, balancing between forest biome internal homogeneity on the one and inter-biome dissimilarity on the other hand (Figure A7).

Our way to calculate BioCol differs substantially from previous approaches for HANPP. First, our calculation is exclusively based on model output, with the aim to also simulate future scenarios and historical periods outside of available biomass inventory data. But we also use a different baseline, when comparing to the static preindustrial NPP and taking the absolute of cells with negative HANPP values. Both is done deliberately in order to ~~1~~(i) not let ourselves get distracted from the fact that global NPP is mainly rising because the biosphere is in a resilience response phase to increasing atmospheric CO_2 levels, meaning that this additional NPP is not ours to use, and ~~2~~(ii) acknowledge that management driven NPP increases beyond the potential natural values (negative NPP_{luc}) usually go together with modification of the water, carbon, or nitrogen cycles stressing local ecosystems.

The underlying principle of BioCol, NPP appropriation, is a function of human demand, i.e. land use change, and biomass harvesting for food, fiber, fodder, bioenergy and bioeconomy. It is therefore closely associated with issues not just of Earth system stability but also of justice, access, and sustainable management of resources (see Gupta et al. 2023). The challenge is to maintain the productivity of the biosphere, i.e. the sustainably available NPP, while ensuring the stability of the biosphere, and beyond that, including climate and the ecosphere, i.e. the Earth system as used by humans.

Complementary, EcoRisk indicates where and when critical transitions in ecosystems occur (as a result of NPP appropriation, but also from climate change, or other environmental pollution). It is thus a very useful indicator to assess the risk of ecosystem destabilization today and also forward, depending on which pathway humanity will take in the future. We deliberately call it a risk metric, because the mathematical property of measuring a non-directional change for us directly translates to a proxy for the risk of ecosystem destabilization. Of course, there could be regions, where ecosystems can benefit from changing biogeochemical properties, however we would argue that when comparing to a long-term stable, land use free preindustrial reference situation (like the Holocene), most ecosystems would be at the risk of being thrown out of this equilibrium when presented with changing conditions. This choice of reference might need to be changed for application of EcoRisk to future climate stabilization scenarios with "Earth-System Stewardship" (Rockström et al., 2021; Steffen et al., 2018).

5 Conclusions

Humanity faces the challenge to stabilize the Earth System in the Anthropocene. This requires stabilizing the climate as well as ~~a~~ maintaining a resilient biosphere, which represents, according to Steffen et al. (2015), a key pillar of the Earth system. We here present two computable biosphere integrity indicators which allow to assess historical and future risk of biosphere destabilization. These are designed to complement other biosphere integrity indicators.

Human appropriation of NPP is a direct result of land-use changes, modulated by climatic changes, irrigation, fertilization and other management, leading to biosphere integrity loss that can be measured by EcoRisk. On the other hand, also natural

NPP is modified by changes in climate, water availability, biosphere integrity, and human land-use. Thus, BioCol and EcoRisk are metrics which integrate multiple terrestrial planetary boundaries (Rockström et al., 2009; Steffen et al., 2015) and human drivers into two numbers, comparable to what global mean temperature does for the underlying, more complex climate processes. Therefore, BioCol and EcoRisk have the potential to be included as indicators in an updated planetary boundaries
350 framework. While well-established as a concept, there so far has been no simulation model for assessing and projecting HANPP on the global scale, to for example analyze future scenarios not accessible through inventory data.

Both BioCol and EcoRisk are spatially explicit, process-based, computable metrics that can be aggregated over space and time. They can therefore serve as integrative meta-level proxies for biosphere integrity and Earth system stability and their dynamic changes. The code used here for their calculation is distributed as an open source R-package and we invite external
355 contributions. With the next update, we plan to equip it to deal with netcdf files, a common data exchange format for spatial data, which allows for future application to different models. Thereby, we hope to encourage others to join our quest to better understand the role of ecosystems for Earth system stability and find ways of how to preserve it.

Code and data availability. The package is available via github https://github.com/stenzelf/biospheremetrics, permanently archived via zenodo https://doi.org/10.5281/zenodo.10699198. LPJmL model code, simulation data, and scripts to generate the Figures are available on
360 Zenodo https://doi.org/10.5281/zenodo.10008051.
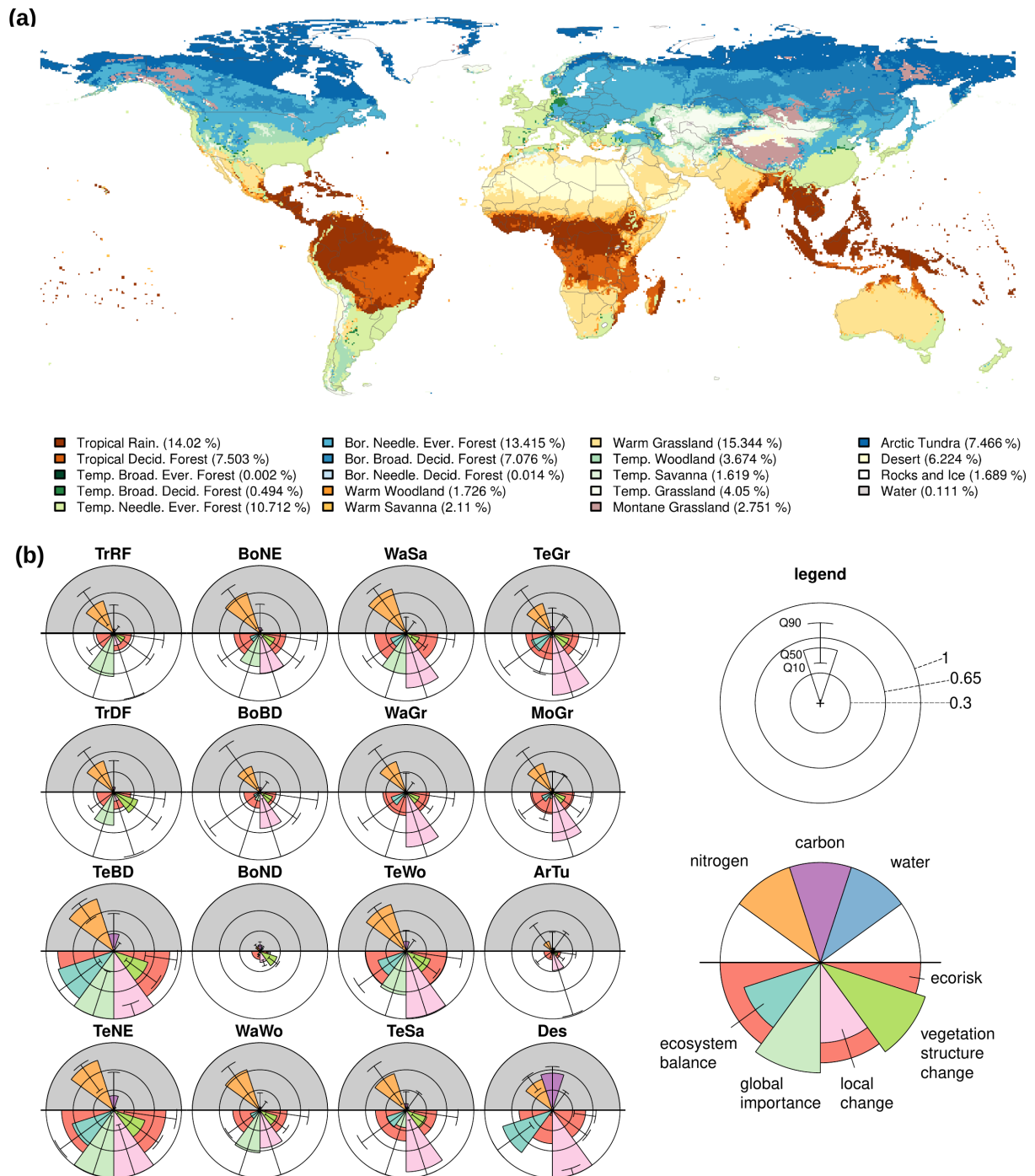
Figure 4. (a) Today's (1987-2016) biomes classified from vegetation structure, plant specific leaf area index, temperature and elevation in LPJmL5. **(b)** Change in biochemical compositions computed by EcoRisk between 1550-1579 and 1985-2016 as the median (Q10 and Q90 for whiskers) across the 16 most relevant biomes ("Temperate Broadleaved Evergreen Forest" basically does not establish – only 2 cells are classified as such – "Rocks and Ice" as well as "Water" skipped for lack of vegetation). For table with biome names and abbreviations see Table A1.
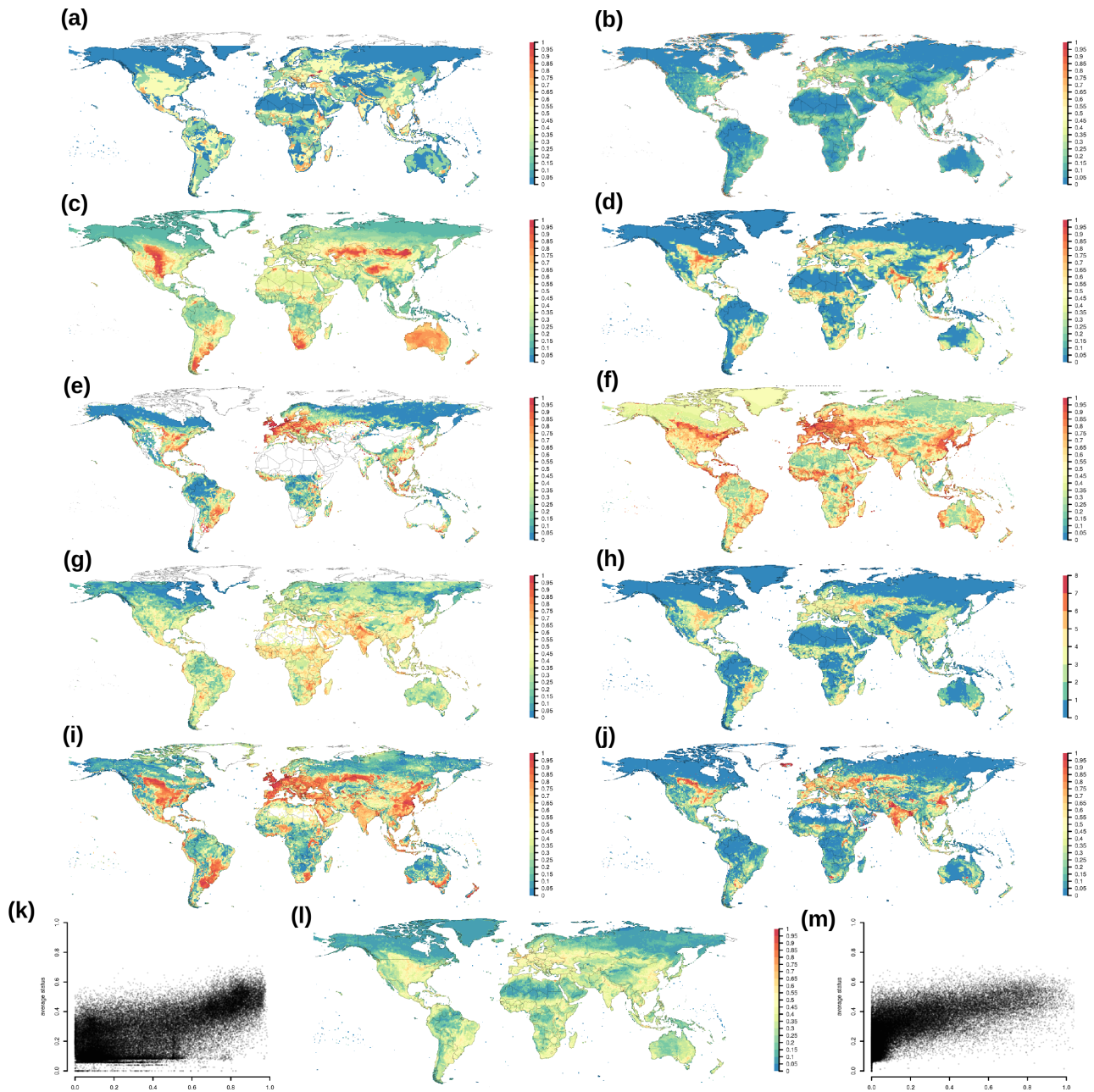
Figure 5. Contextualization of several indicators of biosphere integrity, transformed to the interval [0,1], with 0 meaning high integrity/no pressure/low risk. **(a)** GLASOD: human induced soil degradation (Oldeman et al., 1990), **(b)** HF: human footprint (Venter et al., 2016), **(c)** BII: biodiversity intactness index (Newbold et al., 2016), **(d)** intactness: GLOBIOM 2015 MSA (Schipper et al., 2020), **(e)** FLII: Forest Landscape Intactness Index (Grantham et al., 2020), **(f)** CI: contextual intactness (Mokany et al., 2020b), **(g)** CoE: Convergence of Evidence from World Atlas of Desertification (Cherlet et al., 2018). **(h)** number of previous 7 indicators per grid cell that show up as transgressed (see Table 4 for thresholds indicating transition between low and high risk zones), **(i)** EcoRisk and **(j)** BioCol **(l)** average of metrics a-g **(k)** scatterplot EcoRisk vs average, **(m)** scatterplot BioCol vs average.

Table A1. Names and abbreviations for all biomes according to our biome classification.

Biome	Abbreviation
Tropical Rainforest	TrRF
Tropical Seasonal & Deciduous Forest	TrDF
Temperate Broadleaved Evergreen Forest	TeBE
Temperate Broadleaved Deciduous Forest	TeBD
Temperate Needleleaved Evergreen Forest	TeNE
Boreal Needleleaved Evergreen Forest	BoNE
Boreal Broadleaved Deciduous Forest	BoBD
Boreal Needleleaved Deciduous Forest	BoND
Warm Woody Savanna, Woodland & Shrubland	WaWo
Warm Savanna & Open Shrubland	WaSa
Warm Grassland	WaGr
Temperate Woody Savanna, Woodland & Shrubland	TeWo
Temperate Savanna & Open Shrubland	TeSa
Temperate Grassland	TeGr
Montane Grassland	MoGr
Arctic Tundra	ArTu
Desert	Des
Rocks and Ice	RoIc
Water	Wat
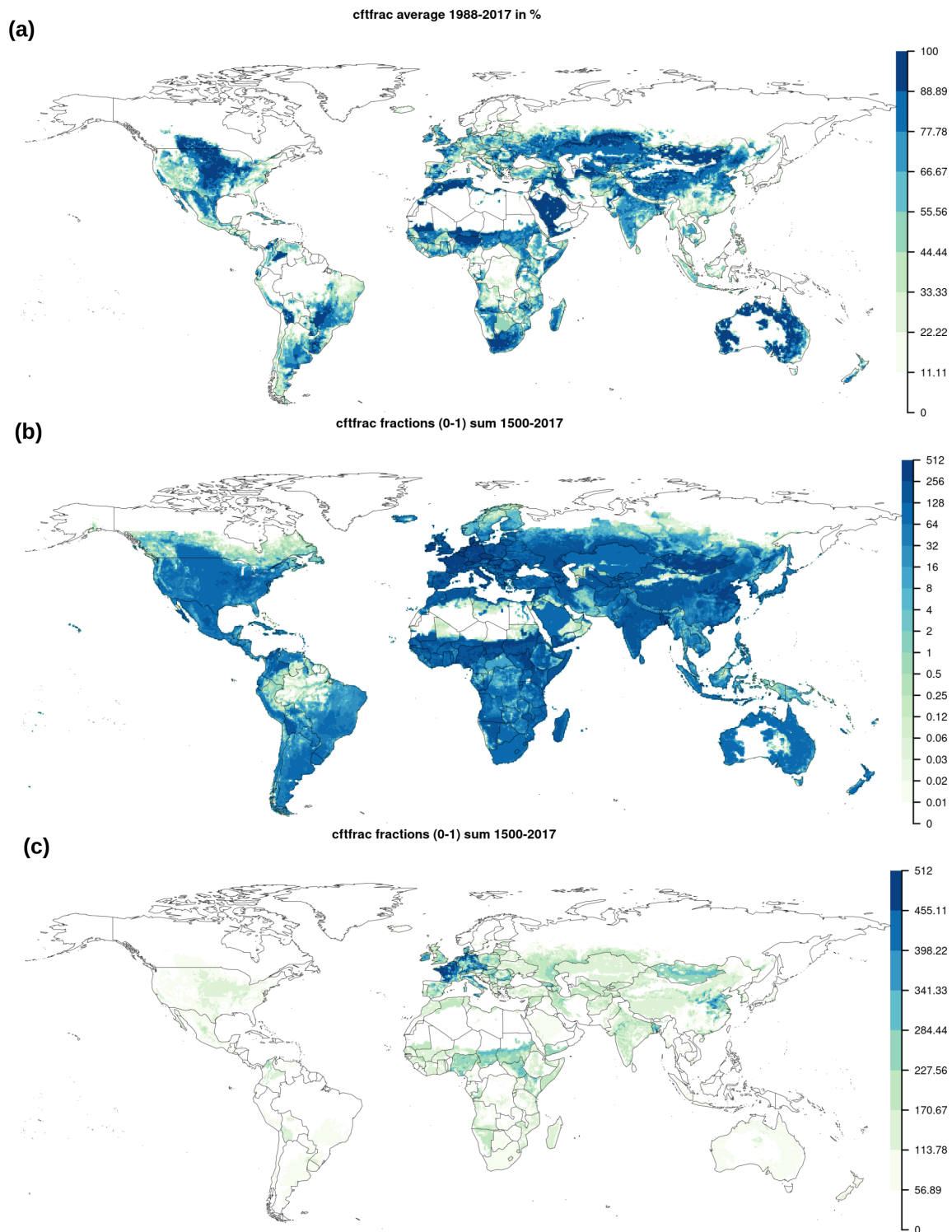
Figure A1. (a) Average land use between 1988-2017 in % of grid cell area. **(b)** Total historical sum of yearly land use fractions [0-1] with exponential, and **(c)** linear legend.
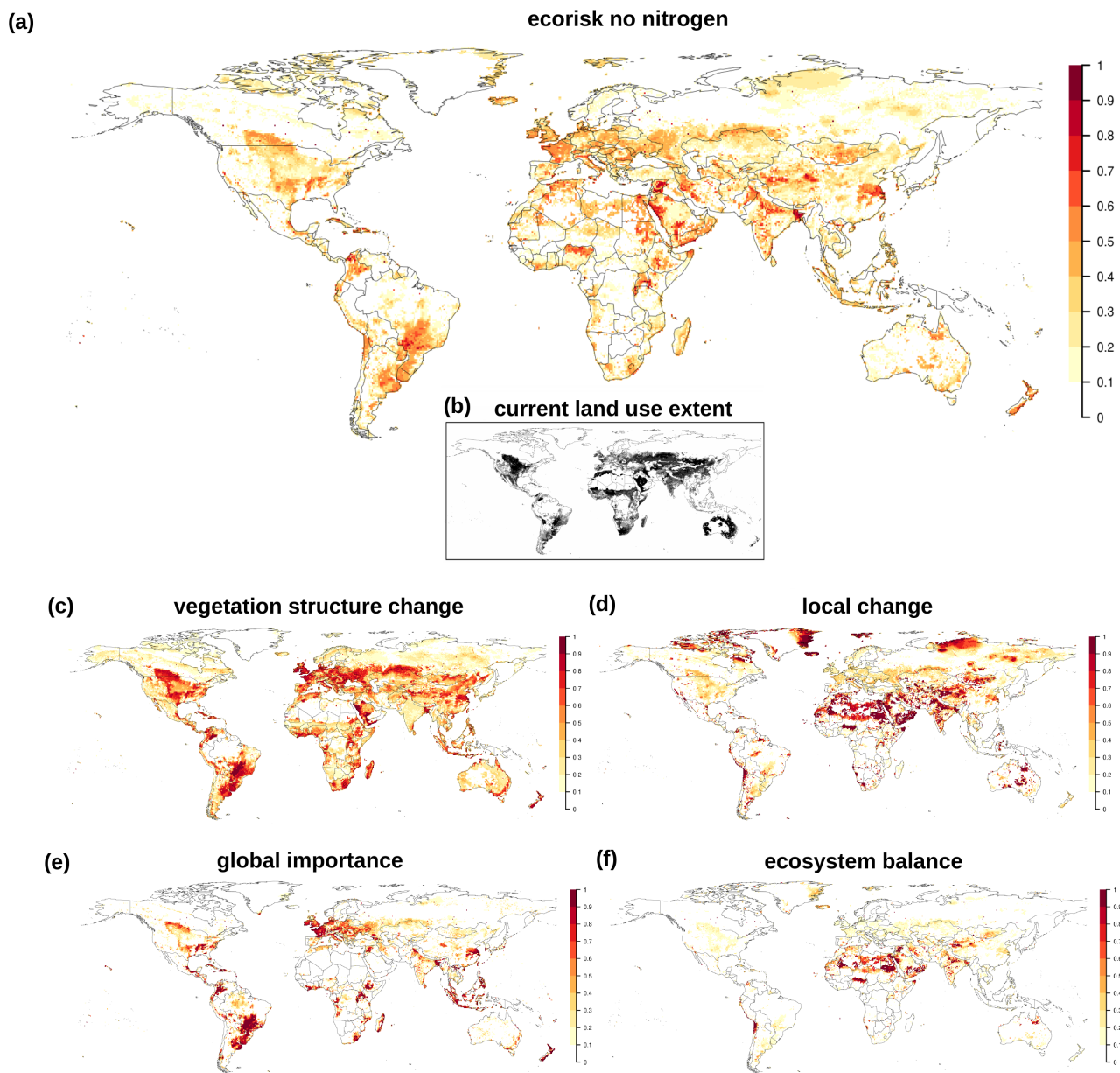
Figure A2. (a) Change in biochemical compositions computed by EcoRisk (as in Figure 3, but excluding Nitrogen variables) between 1550-1579 and 1985-2016. **(b-e)** EcoRisk components: vegetation structure change, local change, global importance, ecosystem balance.
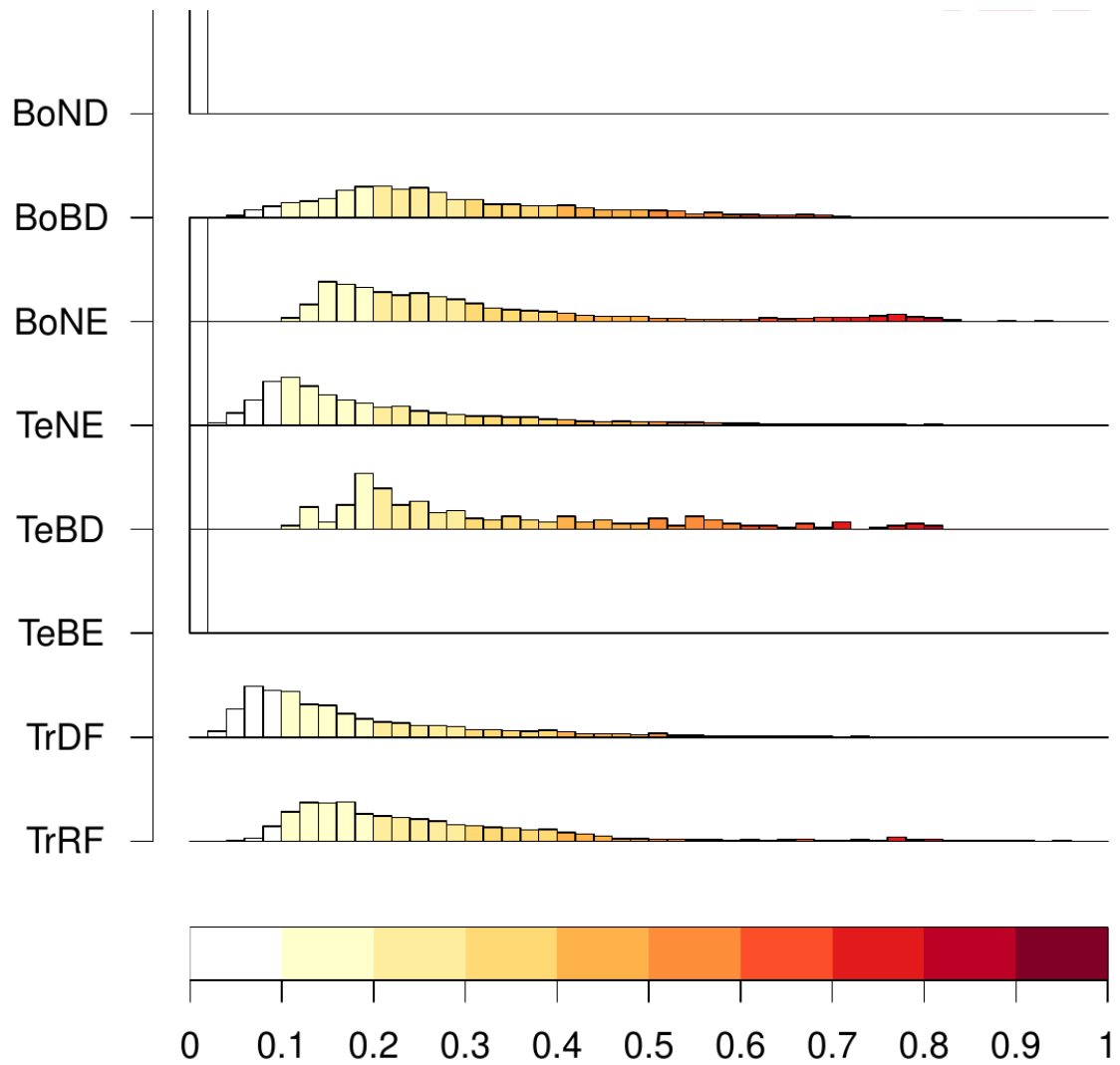
Figure A3. Biome internal difference distribution for the forest biomes computed using EcoRisk between each cell of the biome with the average cell of the biome (for 1550-1579 states). Note that only very few cells are classified as BoND or TeBE - therefore their distribution appears very homogeneous. For biome names and abbreviations see Table A1.

	TrRF	TrDF	TeBD	TeNE	BoNE	BoBD	BoND	WaWo	WaSa	WaGr	TeWo	TeSa	TeGr	MoGr	ArTu	Des
Tropical Rain.	0	0.23	0.7	0.53	0.87	0.88	0.92	0.75	0.95	0.97	0.91	0.95	0.97	0.97	0.96	0.99
Tropical Decid. Forest	0.39	0	0.78	0.75	0.87	0.87	0.91	0.81	0.95	0.97	0.91	0.95	0.97	0.97	0.96	0.99
Temp. Broad. Decid. Forest	0.66	0.65	0	0.47	0.62	0.78	0.84	0.64	0.88	0.86	0.57	0.71	0.89	0.93	0.92	0.98
Temp. Needle. Ever. Forest	0.65	0.62	0.76	0	0.77	0.85	0.89	0.89	0.95	0.97	0.88	0.93	0.96	0.96	0.96	0.99
Bor. Needle. Ever. Forest	0.67	0.67	0.26	0.51	0	0.68	0.86	0.59	0.58	0.61	0.33	0.49	0.76	0.91	0.93	0.97
Bor. Broad. Decid. Forest	0.7	0.7	0.51	0.64	0.53	0	0.47	0.77	0.8	0.72	0.57	0.64	0.79	0.52	0.61	0.98
Bor. Needle. Decid. Forest	0.76	0.76	0.65	0.74	0.67	0.57	0	0.67	0.73	0.7	0.56	0.63	0.78	0.6	0.63	1
Warm Woodland	0.76	0.77	0.75	0.8	0.79	0.88	0.82	0	0.69	0.85	0.66	0.75	0.89	0.88	0.87	0.99
Warm Savanna	0.89	0.9	0.77	0.87	0.75	0.79	0.82	0.34	0	0.68	0.54	0.54	0.87	0.77	0.8	0.98
Warm Grassland	0.93	0.94	0.77	0.93	0.82	0.83	0.85	0.66	0.52	0	0.52	0.32	0.24	0.72	0.76	0.78
Temp. Woodland	0.74	0.75	0.38	0.72	0.5	0.82	0.79	0.53	0.63	0.48	0	0.14	0.67	0.85	0.85	0.93
Temp. Savanna	0.87	0.88	0.65	0.87	0.71	0.84	0.85	0.62	0.59	0.36	0.26	0	0.59	0.79	0.81	0.88
Temp. Grassland	0.97	0.97	0.86	0.96	0.9	0.87	0.82	0.73	0.69	0.38	0.63	0.49	0	0.75	0.75	0.63
Montane Grassland	0.88	0.89	0.81	0.89	0.83	0.68	0.52	0.73	0.69	0.49	0.68	0.61	0.51	0	0.08	0.91
Arctic Tundra	0.87	0.87	0.8	0.88	0.82	0.7	0.58	0.75	0.75	0.64	0.68	0.65	0.5	0.12	0	0.88
Desert	0.99	0.99	0.98	0.99	0.99	0.96	0.99	0.93	0.91	0.72	0.91	0.83	0.6	0.93	0.91	0

Figure A4. Comparison of the state difference (EcoRisk) between biomes according to the average biome cell (y: reference state, x: scenario state) evaluated for the average state of 1550-1579. The colorcode is the same as in Figure A3. Since only very few cells are classified as TeBE, this biome is left out. Biomes RoIce and Wat do not host vegetation and are also left out. For biome names and abbreviations see Table A1.
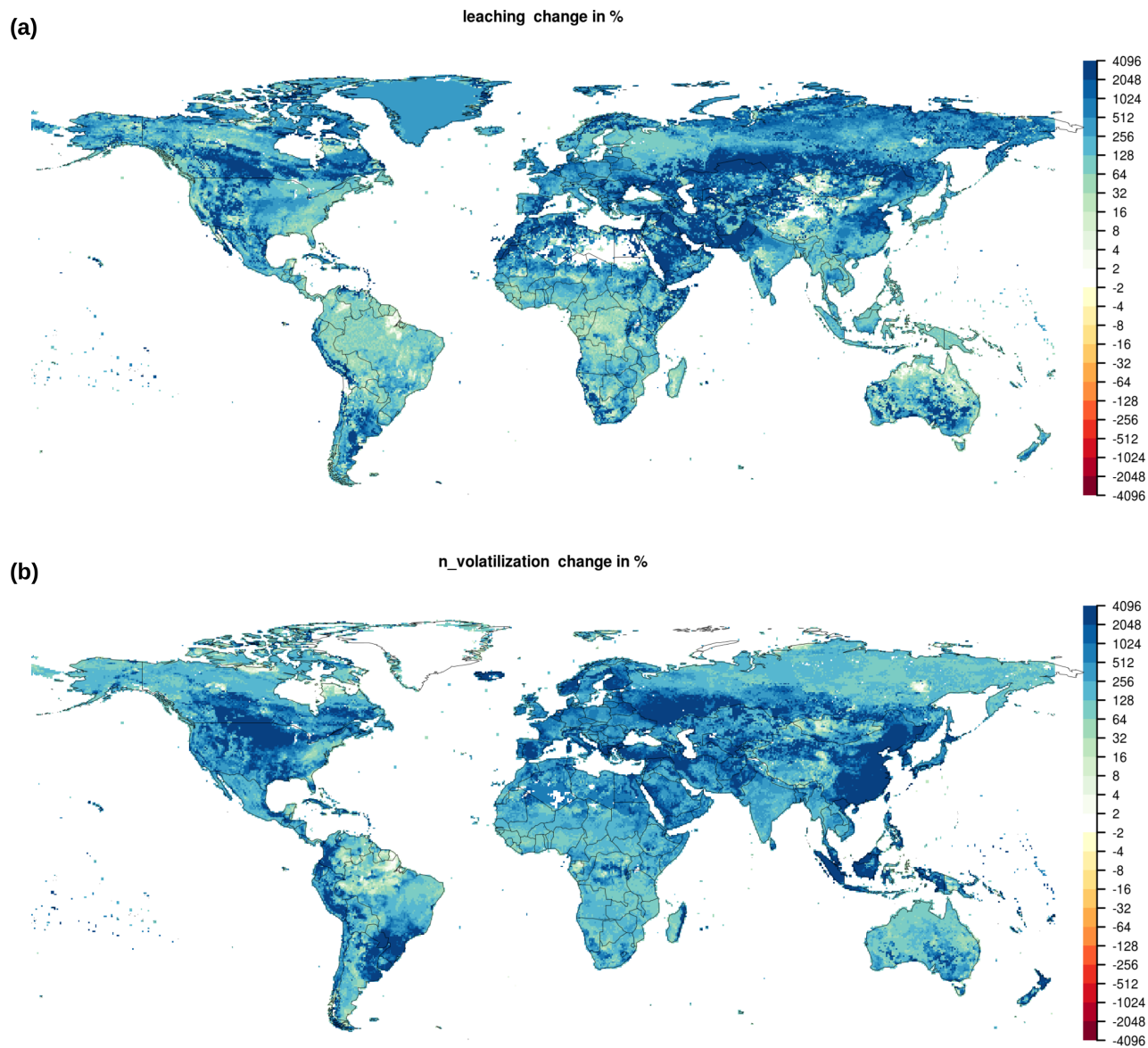
Figure A5. Change in **(a)** leaching and **(b)** nitrogen volatilization between 1550-1579 and 1985-2016
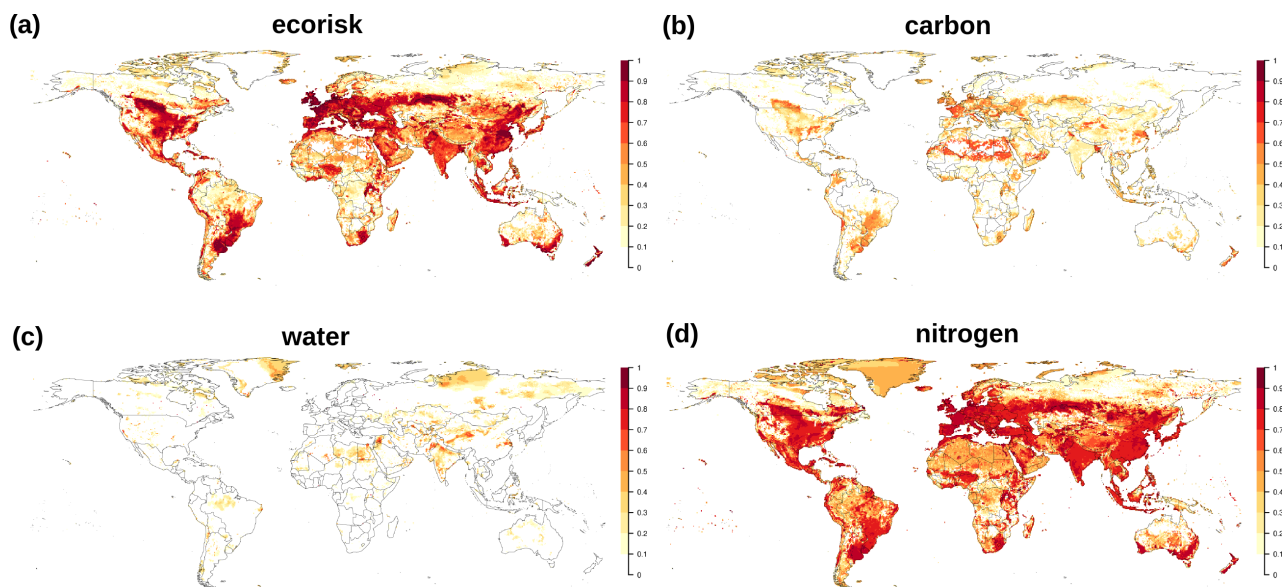
Figure A6. Change in biochemical compositions computed by EcoRisk between 1550-1579 and 1985-2016. **(a)** total ecorisk, and an evaluation of (gi+lc+eb)/3 only for components related to **(b)** carbon, **(c)** water, **(d)** nitrogen.
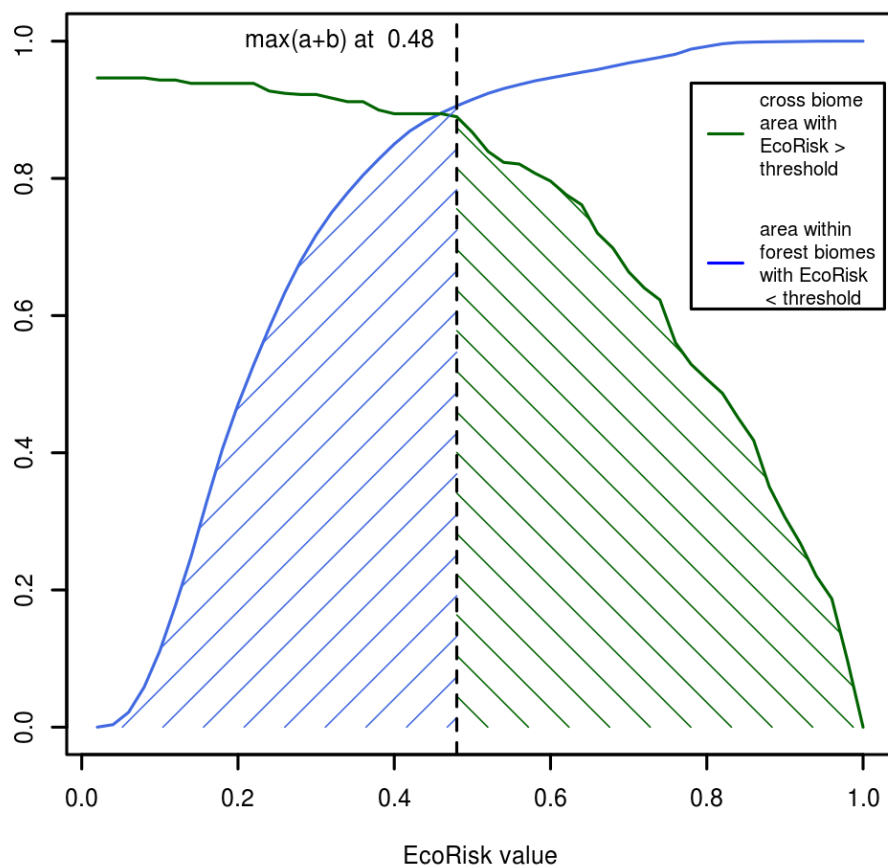
Figure A7. Cumulative area for all cells defined as not similar (Ecorisk > threshold) according to Figure A4 (green), and defined as similar (EcoRisk < threshold) to the biome average according to Figure A3 (blue). The value where the sum of both curves is maximal (an optimal threshold value fulfilling both criteria) is indicated by the dashed vertical line.

Author contributions. FS: Conceptualization, Methodology, Software, Validation, Formal analysis, Writing - Original Draft, Visualization; JoB: Methodology, Software, Writing - Review & Editing; JaB: Software, Writing - Review & Editing; KE: Methodology, Writing - Review & Editing; DG: Writing - Review & Editing, Supervision; JH: Software (livestock-grassland calibration implementation); SM: Methodology, Data Curation, Writing - Review & Editing; SO: Methodology, Software, Writing - Review & Editing; SS: Conceptualization, Data Curation, Writing - Review & Editing; WL: Conceptualization, Writing - Review & Editing, Supervision, Funding acquisition

Competing interests. The authors declare no competing interests.

Acknowledgements. We thank the *Ecosystem in Transitions* group at PIK and especially Boris Sakschewski for fruitful discussions. FS is funded by the Global Challenges Foundation via Future Earth.

365

References

370 Aragão, L. E. O. C.: The rainforest's water pump, Nature, 489, 217–218, https://doi.org/10.1038/nature11485, 2012.

Arneth, A., Denton, F., Agus, F., Elbehri, A., Erb, K., Osman Elasha, B., Rahimi, M., Rounsevell, M., Spence, A., Valentini, R., and Debonne, N.: Framing and Context, pp. 77–129, Intergovernmental Panel on Climate Change (IPCC), https://research.vu.nl/en/publications/framing-and-context, 2019.

Belward, A. S.: The IGBP-DIS Global 1 Km Land Cover Data Set "DISCover": Proposal and Implementation Plans: Report of the Land
375 Recover Working Group of IGBP-DIS, IGBP-DIS, 1996.

Beringer, T., Lucht, W., and Schaphoff, S.: Bioenergy production potential of global biomass plantations under environmental and agricultural constraints, GCB Bioenergy, 3, 299–312, https://doi.org/10.1111/j.1757-1707.2010.01088.x, 2011.

Bondeau, A., Smith, P. C., Zaehle, S., Schaphoff, S., Lucht, W., Cramer, W., Gerten, D., Lotze-Campen, H., Müller, C., Reichstein, M., and Smith, B.: Modelling the role of agriculture for the 20th century global terrestrial carbon balance, Global Change Biology, 13, 679–706,
380 https://doi.org/10.1111/j.1365-2486.2006.01305.x, 2007.

Breier, J., Ostberg, S., Wirth, S. B., Minoli, S., Stenzel, F., and Müller, C.: lpjmlkit: Toolkit for Basic LPJmL Handling, https://github.com/PIK-LPJmL/lpjmlkit, https://doi.org/10.5281/zenodo.7773134, 2023.

Cherlet, M., Hutchinson, C., Reynolds, J., Hill, J., Sommer, S., and Von Maltitz, G. E.: World atlas of desertification: rethinking land degradation and sustainable land management, Publication Office of the European Union, Luxembourg, https://data.europa.eu/doi/10.
385 2760/06292, 2018.

Drüke, M., Bloh, W. v., Sakschewski, B., Wunderling, N., Petri, S., Cardoso, M., Barbosa, H. M. J., and Thonicke, K.: Climate-induced hysteresis of the tropical forest in a fire-enabled Earth system model, The European Physical Journal Special Topics, https://doi.org/10.1140/epjs/s11734-021-00157-2, 2021.

Friedlingstein, P., O'Sullivan, M., Jones, M. W., Andrew, R. M., Gregor, L., Hauck, J., Le Quéré, C., Luijkx, I. T., Olsen, A., Peters, G. P.,
390 Peters, W., Pongratz, J., Schwingshackl, C., Sitch, S., Canadell, J. G., Ciais, P., Jackson, R. B., Alin, S. R., Alkama, R., Arneth, A., Arora, V. K., Bates, N. R., Becker, M., Bellouin, N., Bittig, H. C., Bopp, L., Chevallier, F., Chini, L. P., Cronin, M., Evans, W., Falk, S., Feely, R. A., Gasser, T., Gehlen, M., Gkritzalis, T., Gloege, L., Grassi, G., Gruber, N., Gürses, O., Harris, I., Hefner, M., Houghton, R. A., Hurtt, G. C., Iida, Y., Ilyina, T., Jain, A. K., Jersild, A., Kadono, K., Kato, E., Kennedy, D., Klein Goldewijk, K., Knauer, J., Korsbakken, J. I., Landschützer, P., Lefèvre, N., Lindsay, K., Liu, J., Liu, Z., Marland, G., Mayot, N., McGrath, M. J., Metzl, N., Monacci, N. M., Munro,
395 D. R., Nakaoka, S.-I., Niwa, Y., O'Brien, K., Ono, T., Palmer, P. I., Pan, N., Pierrot, D., Pocock, K., Poulter, B., Resplandy, L., Robertson, E., Rödenbeck, C., Rodriguez, C., Rosan, T. M., Schwinger, J., Séférian, R., Shutler, J. D., Skjelvan, I., Steinhoff, T., Sun, Q., Sutton, A. J., Sweeney, C., Takao, S., Tanhua, T., Tans, P. P., Tian, X., Tian, H., Tilbrook, B., Tsujino, H., Tubiello, F., van der Werf, G. R., Walker, A. P., Wanninkhof, R., Whitehead, C., Willstrand Wranne, A., Wright, R., Yuan, W., Yue, C., Yue, X., Zaehle, S., Zeng, J., and Zheng, B.: Global Carbon Budget 2022, Earth System Science Data, 14, 4811–4900, https://doi.org/10.5194/essd-14-4811-2022, 2022.

400 Gerten, D., Schaphoff, S., Haberlandt, U., Lucht, W., and Sitch, S.: Terrestrial vegetation and water balance—hydrological evaluation of a dynamic global vegetation model, Journal of Hydrology, 286, 249–270, https://doi.org/10.1016/j.jhydrol.2003.09.029, 2004.

Grantham, H. S., Duncan, A., Evans, T. D., Jones, K. R., Beyer, H. L., Schuster, R., Walston, J., Ray, J. C., Robinson, J. G., Callow, M., Clements, T., Costa, H. M., DeGemmis, A., Elsen, P. R., Ervin, J., Franco, P., Goldman, E., Goetz, S., Hansen, A., Hofsvang, E., Jantz, P., Jupiter, S., Kang, A., Langhammer, P., Laurance, W. F., Lieberman, S., Linkie, M., Malhi, Y., Maxwell, S., Mendez, M., Mittermeier, R.,
405 Murray, N. J., Possingham, H., Radachowsky, J., Saatchi, S., Samper, C., Silverman, J., Shapiro, A., Strassburg, B., Stevens, T., Stokes, E.,

Taylor, R., Tear, T., Tizard, R., Venter, O., Visconti, P., Wang, S., and Watson, J. E. M.: Anthropogenic modification of forests means only 40% of remaining forests have high ecosystem integrity, Nature Communications, 11, 5978, https://doi.org/10.1038/s41467-020-19493-3, 2020.

Gupta, J., Liverman, D., Prodani, K., Aldunce, P., Bai, X., Broadgate, W., Ciobanu, D., Gifford, L., Gordon, C., Hurlbert, M., Inoue, C. Y. A., Jacobson, L., Kanie, N., Lade, S. J., Lenton, T. M., Obura, D., Okereke, C., Otto, I. M., Pereira, L., Rockström, J., Scholtens, J., Rocha, J., Stewart-Koster, B., David Tàbara, J., Rammelt, C., and Verburg, P. H.: Earth system justice needed to identify and live within Earth system boundaries, Nature Sustainability, pp. 1–9, https://doi.org/10.1038/s41893-023-01064-1, 2023.

Haberl, H., Erb, K.-H., Krausmann, F., and Lucht, W.: Defining the human appropriation of net primary production, LUCC Newsletter, 10, 16–17, 2004.

Haberl, H., Erb, K. H., Krausmann, F., Gaube, V., Bondeau, A., Plutzar, C., Gingrich, S., Lucht, W., and Fischer-Kowalski, M.: Quantifying and mapping the human appropriation of net primary production in earth's terrestrial ecosystems, Proceedings of the National Academy of Sciences, 104, 12 942–12 947, https://doi.org/10.1073/pnas.0704243104, 2007.

Haberl, H., Erb, K.-H., and Krausmann, F.: Human Appropriation of Net Primary Production: Patterns, Trends, and Planetary Boundaries, Annual Review of Environment and Resources, 39, 363–391, https://doi.org/10.1146/annurev-environ-121912-094620, 2014.

Harper, K. L., Lamarche, C., Hartley, A., Peylin, P., Ottlé, C., Bastrikov, V., San Martín, R., Bohnenstengel, S. I., Kirches, G., Boettcher, M., Shevchuk, R., Brockmann, C., and Defourny, P.: A 29-year time series of annual 300 m resolution plant-functional-type maps for climate models, Earth System Science Data, 15, 1465–1499, https://doi.org/10.5194/essd-15-1465-2023, 2023.

Heinke, J., Lannerstad, M., Gerten, D., Havlík, P., Herrero, M., Notenbaert, A. M. O., Hoff, H., and Müller, C.: Water Use in Global Livestock Production—Opportunities and Constraints for Increasing Water Productivity, Water Resources Research, 56, https://doi.org/10.1029/2019WR026995, 2020.

Heinke, J., Rolinski, S., and Müller, C.: Modelling the role of livestock grazing in C and N cycling in grasslands with LPJmL5.0-grazing, Geoscientific Model Development, 16, 2455–2475, https://doi.org/10.5194/gmd-16-2455-2023, 2023.

Herrero, M., Havlík, P., Valin, H., Notenbaert, A., Rufino, M. C., Thornton, P. K., Blümmel, M., Weiss, F., Grace, D., and Obersteiner, M.: Biomass use, production, feed efficiencies, and greenhouse gas emissions from global livestock systems, Proceedings of the National Academy of Sciences, 110, 20 888–20 893, https://doi.org/10.1073/pnas.1308149110, 2013.

Heyder, U., Schaphoff, S., Gerten, D., and Lucht, W.: Risk of severe climate change impact on the terrestrial biosphere, Environmental Research Letters, 6, 034 036, https://doi.org/10.1088/1748-9326/6/3/034036, 2011.

Hof, C., Voskamp, A., Biber, M. F., Böhning-Gaese, K., Engelhardt, E. K., Niamir, A., Willis, S. G., and Hickler, T.: Bioenergy cropland expansion may offset positive effects of climate change mitigation for global vertebrate diversity, Proceedings of the National Academy of Sciences, 115, 13 294–13 299, https://doi.org/10.1073/pnas.1807745115, 2018.

Hudson, L. N., Newbold, T., Contu, S., Hill, S. L. L., Lysenko, I., De Palma, A., Phillips, H. R. P., Alhusseini, T. I., Bedford, F. E., Bennett, D. J., Booth, H., Burton, V. J., Chng, C. W. T., Choimes, A., Correia, D. L. P., Day, J., Echeverría-Londoño, S., Emerson, S. R., Gao, D., Garon, M., Harrison, M. L. K., Ingram, D. J., Jung, M., Kemp, V., Kirkpatrick, L., Martin, C. D., Pan, Y., Pask-Hale, G. D., Pynegar, E. L., Robinson, A. N., Sanchez-Ortiz, K., Senior, R. A., Simmons, B. I., White, H. J., Zhang, H., Aben, J., Abrahamczyk, S., Adum, G. B., Aguilar-Barquero, V., Aizen, M. A., Albertos, B., Alcala, E. L., del Mar Alguacil, M., Alignier, A., Ancrenaz, M., Andersen, A. N., Arbeláez-Cortés, E., Armbrecht, I., Arroyo-Rodríguez, V., Aumann, T., Axmacher, J. C., Azhar, B., Azpiroz, A. B., Baeten, L., Bakayoko, A., Báldi, A., Banks, J. E., Baral, S. K., Barlow, J., Barratt, B. I. P., Barrico, L., Bartolommei, P., Barton, D. M., Basset, Y., Batáry, P., Bates, A. J., Baur, B., Bayne, E. M., Beja, P., Benedick, S., Berg, A., Bernard, H., Berry, N. J., Bhatt, D., Bicknell, J. E., Bihn, J. H.,

Blake, R. J., Bobo, K. S., Bóçon, R., Boekhout, T., Böhning-Gaese, K., Bonham, K. J., Borges, P. A. V., Borges, S. H., Boutin, C., Bouyer,
J., Bragagnolo, C., Brandt, J. S., Brearley, F. Q., Brito, I., Bros, V., Brunet, J., Buczkowski, G., Buddle, C. M., Bugter, R., Buscardo, E.,
Buse, J., Cabra-García, J., Cáceres, N. C., Cagle, N. L., Calviño-Cancela, M., Cameron, S. A., Cancello, E. M., Caparrós, R., Cardoso,
P., Carpenter, D., Carrijo, T. F., Carvalho, A. L., Cassano, C. R., Castro, H., Castro-Luna, A. A., Rolando, C. B., Cerezo, A., Chapman,
K. A., Chauvat, M., Christensen, M., Clarke, F. M., Cleary, D. F., Colombo, G., Connop, S. P., Craig, M. D., Cruz-López, L., Cunningham,
S. A., D'Aniello, B., D'Cruze, N., da Silva, P. G., Dallimer, M., Danquah, E., Darvill, B., Dauber, J., Davis, A. L. V., Dawson, J., de Sassi,
C., de Thoisy, B., Deheuvels, O., Dejean, A., Devineau, J.-L., Diekötter, T., Dolia, J. V., Domínguez, E., Dominguez-Haydar, Y., Dorn,
S., Draper, I., Dreber, N., Dumont, B., Dures, S. G., Dynesius, M., Edenius, L., Eggleton, P., Eigenbrod, F., Elek, Z., Entling, M. H.,
Esler, K. J., de Lima, R. F., Faruk, A., Farwig, N., Fayle, T. M., Felicioli, A., Felton, A. M., Fensham, R. J., Fernandez, I. C., Ferreira,
C. C., Ficetola, G. F., Fiera, C., Filgueiras, B. K. C., Fırıncıoğlu, H. K., Flaspohler, D., Floren, A., Fonte, S. J., Fournier, A., Fowler,
R. E., Franzén, M., Fraser, L. H., Fredriksson, G. M., Freire Jr, G. B., Frizzo, T. L. M., Fukuda, D., Furlani, D., Gaigher, R., Ganzhorn,
J. U., García, K. P., Garcia-R, J. C., Garden, J. G., Garilleti, R., Ge, B.-M., Gendreau-Berthiaume, B., Gerard, P. J., Gheler-Costa, C.,
Gilbert, B., Giordani, P., Giordano, S., Golodets, C., Gomes, L. G. L., Gould, R. K., Goulson, D., Gove, A. D., Granjon, L., Grass, I.,
Gray, C. L., Grogan, J., Gu, W., Guardiola, M., Gunawardene, N. R., Gutierrez, A. G., Gutiérrez-Lamus, D. L., Haarmeyer, D. H., Hanley,
M. E., Hanson, T., Hashim, N. R., Hassan, S. N., Hatfield, R. G., Hawes, J. E., Hayward, M. W., Hébert, C., Helden, A. J., Henden, J.-A.,
Henschel, P., Hernández, L., Herrera, J. P., Herrmann, F., Herzog, F., Higuera-Diaz, D., Hilje, B., Höfer, H., Hoffmann, A., Horgan, F. G.,
Hornung, E., Horváth, R., Hylander, K., Isaacs-Cubides, P., Ishida, H., Ishitani, M., Jacobs, C. T., Jaramillo, V. J., Jauker, B., Hernández,
F. J., Johnson, M. F., Jolli, V., Jonsell, M., Juliani, S. N., Jung, T. S., Kapoor, V., Kappes, H., Kati, V., Katovai, E., Kellner, K., Kessler, M.,
Kirby, K. R., Kittle, A. M., Knight, M. E., Knop, E., Kohler, F., Koivula, M., Kolb, A., Kone, M., Körösi, A., Krauss, J., Kumar, A., Kumar,
R., Kurz, D. J., Kutt, A. S., Lachat, T., Lantschner, V., Lara, F., Lasky, J. R., Latta, S. C., Laurance, W. F., Lavelle, P., Le Féon, V., LeBuhn,
G., Légaré, J.-P., Lehouck, V., Lencinas, M. V., Lentini, P. E., Letcher, S. G., Li, Q., Litchwark, S. A., Littlewood, N. A., Liu, Y., Lo-Man-
Hung, N., López-Quintero, C. A., Louhaichi, M., Lövei, G. L., Lucas-Borja, M. E., Luja, V. H., Luskin, M. S., MacSwiney G, M. C.,
Maeto, K., Magura, T., Mallari, N. A., Malone, L. A., Malonza, P. K., Malumbres-Olarte, J., Mandujano, S., Måren, I. E., Marin-Spiotta,
E., Marsh, C. J., Marshall, E. J. P., Martínez, E., Martínez Pastur, G., Moreno Mateos, D., Mayfield, M. M., Mazimpaka, V., McCarthy,
J. L., McCarthy, K. P., McFrederick, Q. S., McNamara, S., Medina, N. G., Medina, R., Mena, J. L., Mico, E., Mikusinski, G., Milder, J. C.,
Miller, J. R., Miranda-Esquivel, D. R., Moir, M. L., Morales, C. L., Muchane, M. N., Muchane, M., Mudri-Stojnic, S., Munira, A. N.,
Muoñz-Alonso, A., Munyekenye, B. F., Naidoo, R., Naithani, A., Nakagawa, M., Nakamura, A., Nakashima, Y., Naoe, S., Nates-Parra,
G., Navarrete Gutierrez, D. A., Navarro-Iriarte, L., Ndang'ang'a, P. K., Neuschulz, E. L., Ngai, J. T., Nicolas, V., Nilsson, S. G., Noreika,
N., Norfolk, O., Noriega, J. A., Norton, D. A., Nöske, N. M., Nowakowski, A. J., Numa, C., O'Dea, N., O'Farrell, P. J., Oduro, W., Oertli,
S., Ofori-Boateng, C., Oke, C. O., Oostra, V., Osgathorpe, L. M., Otavo, S. E., Page, N. V., Paritsis, J., Parra-H, A., Parry, L., Pe'er, G.,
Pearman, P. B., Pelegrin, N., Pélissier, R., Peres, C. A., Peri, P. L., Persson, A. S., Petanidou, T., Peters, M. K., Pethiyagoda, R. S., Phalan,
B., Philips, T. K., Pillsbury, F. C., Pincheira-Ulbrich, J., Pineda, E., Pino, J., Pizarro-Araya, J., Plumptre, A. J., Poggio, S. L., Politi, N.,
Pons, P., Poveda, K., Power, E. F., Presley, S. J., Proença, V., Quaranta, M., Quintero, C., Rader, R., Ramesh, B. R., Ramirez-Pinilla, M. P.,
Ranganathan, J., Rasmussen, C., Redpath-Downing, N. A., Reid, J. L., Reis, Y. T., Rey Benayas, J. M., Rey-Velasco, J. C., Reynolds, C.,
Ribeiro, D. B., Richards, M. H., Richardson, B. A., Richardson, M. J., Ríos, R. M., Robinson, R., Robles, C. A., Römbke, J., Romero-
Duque, L. P., Rös, M., Rosselli, L., Rossiter, S. J., Roth, D. S., Roulston, T. H., Rousseau, L., Rubio, A. V., Ruel, J.-C., Sadler, J. P., Sáfián,
S., Saldaña-Vázquez, R. A., Sam, K., Samnegård, U., Santana, J., Santos, X., Savage, J., Schellhorn, N. A., Schilthuizen, M., Schmiedel,
U., Schmitt, C. B., Schon, N. L., Schüepp, C., Schumann, K., Schweiger, O., Scott, D. M., Scott, K. A., Sedlock, J. L., Seefeldt, S. S.,

Shahabuddin, G., Shannon, G., Sheil, D., Sheldon, F. H., Shochat, E., Siebert, S. J., Silva, F. A. B., Simonetti, J. A., Slade, E. M., Smith, J., Smith-Pardo, A. H., Sodhi, N. S., Somarriba, E. J., Sosa, R. A., Soto Quiroga, G., St-Laurent, M.-H., Starzomski, B. M., Stefanescu, C., Steffan-Dewenter, I., Stouffer, P. C., Stout, J. C., Strauch, A. M., Struebig, M. J., Su, Z., Suarez-Rubio, M., Sugiura, S., Summerville, K. S., Sung, Y.-H., Sutrisno, H., Svenning, J.-C., Teder, T., Threlfall, C. G., Tiitsaar, A., Todd, J. H., Tonietto, R. K., Torre, I., Tóthmérész, B., Tscharntke, T., Turner, E. C., Tylianakis, J. M., Uehara-Prado, M., Urbina-Cardona, N., Vallan, D., Vanbergen, A. J., Vasconcelos, H. L., Vassilev, K., Verboven, H. A. F., Verdasca, M. J., Verdú, J. R., Vergara, C. H., Vergara, P. M., Verhulst, J., Virgilio, M., Vu, L. V., Waite, E. M., Walker, T. R., Wang, H.-F., Wang, Y., Watling, J. I., Weller, B., Wells, K., Westphal, C., Wiafe, E. D., Williams, C. D., Willig, M. R., Woinarski, J. C. Z., Wolf, J. H. D., Wolters, V., Woodcock, B. A., Wu, J., Wunderle Jr, J. M., Yamaura, Y., Yoshikura, S., Yu, D. W., Zaitsev, A. S., Zeidler, J., Zou, F., Collen, B., Ewers, R. M., Mace, G. M., Purves, D. W., Scharlemann, J. P. W., and Purvis, A.: The database of the PREDICTS (Projecting Responses of Ecological Diversity In Changing Terrestrial Systems) project, Ecology and Evolution, 7, 145–188, https://doi.org/10.1002/ece3.2579, 2017.

Hurtt, G. C., Chini, L., Sahajpal, R., Frolking, S., Bodirsky, B. L., Calvin, K., Doelman, J. C., Fisk, J., Fujimori, S., Klein Goldewijk, K., Hasegawa, T., Havlik, P., Heinimann, A., Humpenöder, F., Jungclaus, J., Kaplan, J. O., Kennedy, J., Krisztin, T., Lawrence, D., Lawrence, P., Ma, L., Mertz, O., Pongratz, J., Popp, A., Poulter, B., Riahi, K., Shevliakova, E., Stehfest, E., Thornton, P., Tubiello, F. N., van Vuuren, D. P., and Zhang, X.: Harmonization of global land use change and management for the period 850–2100 (LUH2) for CMIP6, Geoscientific Model Development, 13, 5425–5464, https://doi.org/10.5194/gmd-13-5425-2020, 2020.

Imhoff, M. L., Bounoua, L., Ricketts, T., Loucks, C., Harriss, R., and Lawrence, W. T.: Global patterns in human consumption of net primary production, Nature, 429, 870–873, https://doi.org/10.1038/nature02619, 2004.

Jägermeyr, J., Gerten, D., Heinke, J., Schaphoff, S., Kummu, M., and Lucht, W.: Water savings potentials of irrigation systems: global simulation of processes and linkages, Hydrol. Earth Syst. Sci., 19, 3073–3091, https://doi.org/10.5194/hess-19-3073-2015, 2015.

Kastner, T., Matej, S., Forrest, M., Gingrich, S., Haberl, H., Hickler, T., Krausmann, F., Lasslop, G., Niedertscheider, M., Plutzar, C., Schwarzmüller, F., Steinkamp, J., and Erb, K.-H.: Land use intensification increasingly drives the spatiotemporal patterns of the global human appropriation of net primary production in the last century, Global Change Biology, 28, 307–322, https://doi.org/https://doi.org/10.1111/gcb.15932, 2022.

Kim, H.: Global Soil Wetness Project Phase 3 (GSWP3) - Atmospheric Boundary Conditions, https://doi.org/10.20783/DIAS.501, 2017.

Krausmann, F., Erb, K.-H., Gingrich, S., Haberl, H., Bondeau, A., Gaube, V., Lauk, C., Plutzar, C., and Searchinger, T. D.: Global human appropriation of net primary production doubled in the 20th century, Proceedings of the National Academy of Sciences, 110, 10 324–10 329, https://doi.org/10.1073/pnas.1211349110, 2013.

Lange, S.: WFDE5 over land merged with ERA5 over the ocean (W5E5). V. 1.0., GFZ Data Services, https://doi.org/10.5880/pik.2019.023, 2019.

Lutz, F., Herzfeld, T., Heinke, J., Rolinski, S., Schaphoff, S., von Bloh, W., Stoorvogel, J. J., and Müller, C.: Simulating the effect of tillage practices with the global ecosystem model LPJmL (version 5.0-tillage), Geoscientific Model Development, 12, 2419–2440, https://doi.org/10.5194/gmd-12-2419-2019, 2019.

McKay, D. I. A., Staal, A., Abrams, J. F., Winkelmann, R., Sakschewski, B., Loriani, S., Fetzer, I., Cornell, S. E., Rockström, J., and Lenton, T. M.: Exceeding 1.5 C global warming could trigger multiple climate tipping points, Science, 377, eabn7950, https://doi.org/10.1126/science.abn7950, 2022.

Mokany, K., Ferrier, S., Harwood, T., Ware, C., Di Marco, M., Grantham, H., Venter, O., Hoskins, A., and Watson, J.: Contextual intactness of habitat for biodiversity: global extent, 30 arcsecond resolution. v1., CSIRO. Data Collection, https://doi.org/https://doi.org/10.25919/5e7854cfcb97e, 2020a.

Mokany, K., Ferrier, S., Harwood, T. D., Ware, C., Marco, M. D., Grantham, H. S., Venter, O., Hoskins, A. J., and Watson, J. E. M.: Reconciling global priorities for conserving biodiversity habitat, Proceedings of the National Academy of Sciences, 117, 9906–9911, https://doi.org/10.1073/pnas.1918373117, 2020b.

Newbold, T., Hudson, L. N., Arnell, A. P., Contu, S., Palma, A. D., Ferrier, S., Hill, S. L. L., Hoskins, A. J., Lysenko, I., Phillips, H. R. P., Burton, V. J., Chng, C. W. T., Emerson, S., Gao, D., Pask-Hale, G., Hutton, J., Jung, M., Sanchez-Ortiz, K., Simmons, B. I., Whitmee, S., Zhang, H., Scharlemann, J. P. W., and Purvis, A.: Has land use pushed terrestrial biodiversity beyond the planetary boundary? A global assessment, Science, 353, 288–291, https://doi.org/10.1126/science.aaf2201, 2016.

Obura, D. O., DeClerck, F., Verburg, P. H., Gupta, J., Abrams, J. F., Bai, X., Bunn, S., Ebi, K. L., Gifford, L., Gordon, C., Jacobson, L., Lenton, T. M., Liverman, D., Mohamed, A., Prodani, K., Rocha, J. C., Rockström, J., Sakschewski, B., Stewart-Koster, B., van Vuuren, D., Winkelmann, R., and Zimm, C.: Achieving a nature- and people-positive future, One Earth, https://doi.org/10.1016/j.oneear.2022.11.013, 2022.

Oldeman, L. R., Hakkeling, R., Sombroek, W. G., et al.: World map of the status of human-induced soil degradation: an explanatory note., International Soil Reference and Information Centre, 1990.

Oliver, T. H., Heard, M. S., Isaac, N. J. B., Roy, D. B., Procter, D., Eigenbrod, F., Freckleton, R., Hector, A., Orme, C. D. L., Petchey, O. L., Proença, V., Raffaelli, D., Suttle, K. B., Mace, G. M., Martín-López, B., Woodcock, B. A., and Bullock, J. M.: Biodiversity and Resilience of Ecosystem Functions, Trends in Ecology & Evolution, 30, 673–684, https://doi.org/10.1016/j.tree.2015.08.009, 2015.

Ostberg, S., Lucht, W., Schaphoff, S., and Gerten, D.: Critical impacts of global warming on land ecosystems, Earth System Dynamics, 4, 347–357, https://doi.org/10.5194/esd-4-347-2013, 2013.

Ostberg, S., Schaphoff, S., Lucht, W., and Gerten, D.: Three centuries of dual pressure from land use and climate change on the biosphere, Environmental Research Letters, 10, 044 011, https://doi.org/10.1088/1748-9326/10/4/044011, 2015.

Ostberg, S., Boysen, L. R., Schaphoff, S., Lucht, W., and Gerten, D.: The Biosphere Under Potential Paris Outcomes, Earth's Future, 6, 23–39, https://doi.org/10.1002/2017EF000628, 2018.

Ostberg, S., Müller, C., Heinke, J., and Schaphoff, S.: LandInG 1.0: A toolbox to derive input datasets for terrestrial ecosystem modelling at variable resolutions from heterogeneous sources, Geoscientific Model Development Discussions, pp. 1–46, https://doi.org/10.5194/gmd-2022-291, 2023.

Porwollik, V., Rolinski, S., Heinke, J., von Bloh, W., Schaphoff, S., and Müller, C.: The role of cover crops for cropland soil carbon, nitrogen leaching, and agricultural yields – a global simulation study with LPJmL (V. 5.0-tillage-cc), Biogeosciences, 19, 957–977, https://doi.org/10.5194/bg-19-957-2022, 2022.

Rockström, J., Steffen, W., Noone, K., Persson, Å., Chapin, F. S., Lambin, E. F., Lenton, T. M., Scheffer, M., Folke, C., Schellnhuber, H. J., Nykvist, B., de Wit, C. A., Hughes, T., van der Leeuw, S., Rodhe, H., Sörlin, S., Snyder, P. K., Costanza, R., Svedin, U., Falkenmark, M., Karlberg, L., Corell, R. W., Fabry, V. J., Hansen, J., Walker, B., Liverman, D., Richardson, K., Crutzen, P., and Foley, J. A.: A safe operating space for humanity, Nature, 461, 472–475, https://doi.org/10.1038/461472a, 2009.

Rockström, J., Beringer, T., Hole, D., Griscom, B., Mascia, M. B., Folke, C., and Creutzig, F.: We need biosphere stewardship that protects carbon sinks and builds resilience, Proceedings of the National Academy of Sciences, 118, e2115218 118, https://doi.org/10.1073/pnas.2115218118, 2021.

Rojstaczer, S., Sterling, S. M., and Moore, N. J.: Human Appropriation of Photosynthesis Products, Science, 294, 2549–2552, https://doi.org/10.1126/science.1064375, 2001.

Sakschewski, B., von Bloh, W., Boit, A., Rammig, A., Kattge, J., Poorter, L., Peñuelas, J., and Thonicke, K.: Leaf and stem economics spectra drive diversity of functional plant traits in a dynamic global vegetation model, Global Change Biology, 21, 2711–2725,

560   https://doi.org/10.1111/gcb.12870, 2015.

Schaphoff, S., von Bloh, W., Rammig, A., Thonicke, K., Biemans, H., Forkel, M., Gerten, D., Heinke, J., Jägermeyr, J., Knauer, J., Langerwisch, F., Lucht, W., Müller, C., Rolinski, S., and Waha, K.: LPJmL4 – a dynamic global vegetation model with managed land – Part 1: Model description, Geoscientific Model Development, 11, 1343–1375, https://doi.org/10.5194/gmd-11-1343-2018, 2018.

Schipper, A. M., Hilbers, J. P., Meijer, J. R., Antão, L. H., Benítez-López, A., de Jonge, M. M. J., Leemans, L. H., Scheper, E., Alkemade,

565   R., Doelman, J. C., Mylius, S., Stehfest, E., van Vuuren, D. P., van Zeist, W.-J., and Huijbregts, M. A. J.: Projecting terrestrial biodiversity intactness with GLOBIO 4, Global Change Biology, 26, 760–771, https://doi.org/10.1111/gcb.14848, 2020.

Sitch, S., Smith, B., Prentice, I. C., Arneth, A., Bondeau, A., Cramer, W., Kaplan, J. O., Levis, S., Lucht, W., Sykes, M. T., Thonicke, K., and Venevsky, S.: Evaluation of ecosystem dynamics, plant geography and terrestrial carbon cycling in the LPJ dynamic global vegetation model, Global Change Biology, 9, 161–185, https://doi.org/10.1046/j.1365-2486.2003.00569.x, 2003.

570   Soergel, B., Kriegler, E., Weindl, I., Rauner, S., Dirnaichner, A., Ruhe, C., Hofmann, M., Bauer, N., Bertram, C., Bodirsky, B. L., Leimbach, M., Leininger, J., Levesque, A., Luderer, G., Pehl, M., Wingens, C., Baumstark, L., Beier, F., Dietrich, J. P., Humpenöder, F., von Jeetze, P., Klein, D., Koch, J., Pietzcker, R., Strefler, J., Lotze-Campen, H., and Popp, A.: A sustainable development pathway for climate action within the UN 2030 Agenda, Nature Climate Change, 11, 656–664, https://doi.org/10.1038/s41558-021-01098-3, 2021.

Steffen, W., Richardson, K., Rockström, J., Cornell, S. E., Fetzer, I., Bennett, E. M., Biggs, R., Carpenter, S. R., Vries, W. d., Wit, C. A. d.,

575   Folke, C., Gerten, D., Heinke, J., Mace, G. M., Persson, L. M., Ramanathan, V., Reyers, B., and Sörlin, S.: Planetary boundaries: Guiding human development on a changing planet, Science, 347, 1259 855, https://doi.org/10.1126/science.1259855, 2015.

Steffen, W., Rockström, J., Richardson, K., Lenton, T. M., Folke, C., Liverman, D., Summerhayes, C. P., Barnosky, A. D., Cornell, S. E., Crucifix, M., Donges, J. F., Fetzer, I., Lade, S. J., Scheffer, M., Winkelmann, R., and Schellnhuber, H. J.: Trajectories of the Earth System in the Anthropocene, Proceedings of the National Academy of Sciences, p. 201810141, https://doi.org/10.1073/pnas.1810141115, 2018.

580   Sykes, M. T., Prentice, I. C., and Laarif, F.: Quantifying the Impact of Global Climate Change on Potential Natural Vegetation, Climatic Change, 41, 37–52, https://doi.org/10.1023/A:1005435831549, 1999.

Thonicke, K., Spessa, A., Prentice, I. C., Harrison, S. P., Dong, L., and Carmona-Moreno, C.: The influence of vegetation, fire spread and fire behaviour on biomass burning and trace gas emissions: results from a process-based model, Biogeosciences, 7, 1991–2011, https://doi.org/10.5194/bg-7-1991-2010, 2010.

585   Venter, O., Sanderson, E. W., Magrach, A., Allan, J. R., Beher, J., Jones, K. R., Possingham, H. P., Laurance, W. F., Wood, P., Fekete, B. M., Levy, M. A., and Watson, J. E. M.: Sixteen years of change in the global terrestrial human footprint and implications for biodiversity conservation, Nature Communications, 7, 12 558, https://doi.org/10.1038/ncomms12558, 2016.

Venter, O., Sanderson, E. W., Magrach, A., Allan, J. R., Beher, J., Jones, K. R., Possingham, H. P., Laurance, W. F., Wood, P., Fekete, B. M., Levy, M. A., and Watson, J. E.: Last of the Wild Project, Version 3 (LWP-3): 2009 Human Footprint, 2018 Release,

590   https://doi.org/10.7927/H46T0JQ4, 2018.

Vitousek, P. M., Ehrlich, P. R., Ehrlich, A. H., and Matson, P. A.: Human appropriation of the products of photosynthesis, BioScience, 36, 368–373, 1986.

von Bloh, W., Schaphoff, S., Müller, C., Rolinski, S., Waha, K., and Zaehle, S.: Implementing the nitrogen cycle into the dynamic global vegetation, hydrology, and crop growth model LPJmL (version 5.0), Geoscientific Model Development, 11, 2789–2812, https://doi.org/10.5194/gmd-11-2789-2018, 2018.

Waha, K., van Bussel, L. G. J., Müller, C., and Bondeau, A.: Climate-driven simulation of global crop sowing dates, Global Ecology and Biogeography, 21, 247–259, https://doi.org/10.1111/j.1466-8238.2011.00678.x, 2012.

Warszawski, L., Friend, A., Ostberg, S., Frieler, K., Lucht, W., Schaphoff, S., Beerling, D., Cadule, P., Ciais, P., Clark, D. B., Kahana, R., Ito, A., Keribin, R., Kleidon, A., Lomas, M., Nishina, K., Pavlick, R., Rademacher, T. T., Buechner, M., Piontek, F., Schewe, J., Serdeczny, O., and Schellnhuber, H. J.: A multi-model analysis of risk of ecosystem shifts under climate change, Environmental Research Letters, 8, 044 018, https://doi.org/10.1088/1748-9326/8/4/044018, 2013.

Watson, J. E. M., Venter, O., Lee, J., Jones, K. R., Robinson, J. G., Possingham, H. P., and Allan, J. R.: Protect the last of the wild, Nature, 563, 27–30, https://doi.org/10.1038/d41586-018-07183-6, 2018.

Weisdorf, J. L.: From Foraging To Farming: Explaining The Neolithic Revolution, Journal of Economic Surveys, 19, 561–586, https://doi.org/10.1111/j.0950-0804.2005.00259.x, 2005.

Williams, D. R., Clark, M., Buchanan, G. M., Ficetola, G. F., Rondinini, C., and Tilman, D.: Proactive conservation to prevent habitat losses to agricultural expansion, Nature Sustainability, 4, 314–322, https://doi.org/10.1038/s41893-020-00656-5, 2021.